# Study and Analysis of SEMG Signal between Elbow and Shoulder using Labview

A thesis submitted in partial fulfillment of the requirements for the award of degree of

**Master of Engineering**
**In**
**Electronic Instrumentation and Control**

Submitted By:
**Ashish Aggarwal**
Roll No. 800951004

Under the Guidance of:
**Dr. Ravinder Aggarwal**
Associate Professor, EIED
Thapar University, Pataiala

**Department of Electrical and Instrumentation Engineering**
**Thapar University, Patiala**
(Established under the section 3 of UGC act, 1956)

Patiala, 147004, Punjab, India

July 2011

## DECLARATION

I hereby certify that the work which is being presented in the thesis entitled, **"Study and Analysis of SEMG signal between elbow and shoulder using Labview"** in partial fulfillment of the requirements for the award of degree of Master of Engineering in Electronic Instrumentation and Control Engineering submitted in Electrical and Instrumentation Engineering, Department of Thapar University, Patiala, is an authentic record of my own work carried out under the supervision of **Dr. Ravinder Aggarwal** (Associate Professor) Department of Electrical and Instrumentation Engineering, Thapar University, Patiala, Punjab.

Date: 14/7/11

**Ashish Aggarwal**

Roll. No. 800951004

I certify that the above statement made by the candidate is correct and true to the best of my knowledge.

Date: 14.07.11

**Dr. Ravinder Aggarwal**
Associate Professor
Department of Electrical and Instrumentation Engineering
Thapar University, Patiala
Punjab

Countersigned By

S. Ghosh 14/7/11

**Dr. Smarajit Ghosh**
Head of Department
Department of Electrical and Instrumentation Engineering
Thapar University, Patiala
Punjab

**Dr. S K Mohapatra**
Dean of Academic Affairs
Thapar University, Patiala
Punjab

# ACKNOWLEDGEMENT

I express my deep sense of gratitude and respects to my guide **Dr. Ravinder Aggarwal**, Associate Professor, Electrical & instrumentation Engineering Department, Thapar University, Patiala for his keen interest and valuable guidance, strong motivation and constant encouragement throughout this thesis work. I thank him for his great patience, constructive criticism and myriad useful suggestions apart from invaluable guidance to me. I am sure that the knowledge gained through my association with my supervisor shall go a long way in helping me to realize my goals in life. I owe my thanks to **Dr. Smarajit Ghosh**, Head of Department of Electrical & Instrumentation engineering for his kind support.

Ashish 14/7/11

**Ashish Aggarwal**

# ABSTRACT

Prosthesis is an artificial extension that replaces a missing body part. Prostheses are typically used to replace parts lost by injury or missing from birth or to supplement defective body parts. In addition to the standard artificial limb for every-day use, many amputees have special limbs and devices to aid in the participation of sports and recreational activities.

Prosthetic arm is a boon for those persons who have lost their arm (below elbow) due some mishap. One of the main requirements of artificial arm is that functionally, it should be as near to the natural hand as possible. Various designs of artificial arm are available in the market, categorized as mechanical, electrical and Myo-electric arm. Mechanical devices are functional prostheses that use some motion of the body to provide the force necessary to control the prosthetic component. Electrical arms operate the hand by a motor driven by micro switches and relays. Myo-Electric arm is stimulated by muscle signal available from the stump of amputee.

In the present research work, SEMG signals were taken by active electrodes between elbow and shoulder with different forces. Signal is acquired in soft scope Labview by DAQ card (NI DAQ 6024E). The SEMG signal at different positions above elbow for various movements like up (m1)/down (m2), clockwise (m3)/anticlockwise (m4) of arm was carried out. After acquiring data from different locations above elbow with different forces, analysis were made using RMS values, standard deviation, power spectrum, time frequency distributions (WVD, CWD).

# Table of Contents

# List of Figures

# List of Tables

# Abbreviations

P1 – first acupressure point

P2 – second acupressure point

m1 – first motion (move arm up)

m2 – second motion (move arm down)

m3 – third motion (move arm clockwise (cw))

m4 – fourth motion (move arm anti-clockwise (acw))

ww – without weight (without force gripper)

WVD - wigner ville distribution

CWD - choi willa distribution

# 1. INTRODUCTION

The history of prosthetic parts is a long one. In medieval times, knights would have prosthetic hands made by their armourers. Over the centuries, the pace of development has been limited not only by technological progress, but also by the small number of people who actually survived the trauma of the amputation and the subsequent risk of infection. In the United States 41,000 persons are registered who had an amputation of a hand or a complete arm. With the same frequency of occurrence (1 in 6100) there would be 1000000 such persons worldwide. The main factors for a loss of an upper extremity are accidents followed by general diseases and injuries from war. Therefore, in last 3 decades an increasing number of handicapped persons have been provided with prosthetic hands that have the shape of a human hand and that are actuated by a DC motor with reduction gear trains.

However, surveys on using such artificial hands revealed that 30 to 50% of the handicapped persons do not use their prosthetic hand regularly. The main factors of the rejection of conventional prosthetic hands were:

- Heavy weight: although commercial prosthetic hands have about the same mass as human hands they appear to be unpleasantly heavy because the mass is transmitted by a lever arm to the short stump of the amputated arm.
- Low functionality: Conventional prosthetic hands can only perform a single pincer-like grip movement. Therefore the gripping abilities are restricted, so it is for example impossible to pick up a pinball with the artificial hand. The fingers have only one degree of freedom and can not adapt to the shape of an object. The consequence is reduced force, which is necessary to hold an object stable.
- Robot-like movement: The movements to appear unnatural.

To overcome these problems lot of efforts have been done worldwide. Research activities improved the functional range of an electrically driven prosthetic arm. As a consequence of the heavy actuators and mechanical elements used in the prosthetic hand has not been reduced [1].

In the body movement, the complex and nonlinear information processing is done from the brain to the body limbs. Human body movement is controlled by the central nervous system in the brain. Motor command firstly is sent from the nervous system to each muscle via motor neurons. It activates the muscles and causes the muscle tensions.

Secondly, the muscle tensions act on the related joint and cause the joint torque. Finally, the joint torque realizes the motion corresponding to the joint dynamics. In the case of amputee, a part of this information processing flow is cut off. It is inconvenient for them to live a daily life. For the expansion and the improvement of amputee's activity of daily living, several kinds of electromyogram (EMG) controlled prosthetic hands have been developed. The use of EMG signals to control the prosthetic hand provides the amputees with a control feeling similar to moving their normal hand.

Actuators and mechanisms research area has shown steadily growing technological advances in externally activated prostheses. The advances include the use of piezoelectric materials, special metal alloys, polymers and new motor applications, while the advances in mechanisms also include mechanical designs based on the anatomy of the human hand and improvements in the way these components are combined. It can be simple artificial limb looks like a human limb called as cosmatic prosthesis, which is made up of latex or silicon but is not able to perform any activity.

It can be used to hide distorted image of an amputee. Another type is a robotic structure of human hand whose control is from switches. Control cables are operated through shoulder's movement, mouth, chest, other hand etc. called body powered prosthesis. In this case specified operations can be performed. Usually small motor provide functions of hand and control is being done through proper sensing of movements of muscles called myo-electric controlled or Electrically powered Prosthesis. Comparisons of these devices are made with regard to the main criteria of construction and operation required to achieve optimal prosthetic performance. The multiple tasks can be performed with electrically powered system.

A myoelectric signal called a motor action potential is an electrical impulse that produces contraction of muscle fibers in the body. The term is most often used in reference to skeletal muscles that control movements. Myoelectric signals are detected by placing three electrodes on the skin. Two electrodes are positioned to measure differential voltage between them when a myoelectric signal occurs. The third electrode is placed in a neutral area and its output is used to cancel the noise that can otherwise interfere with the signals from the other two electrodes. The output of the amplifier has much higher voltage than the myoelectric signals themselves. This higher voltage, which produces significant current, is used to control electromechanical or electronic devices. This signal is normally a function of time and is describable in terms of its amplitude, frequency and phase.

EMG signal is a measure of electrical currents generated in muscles during its contraction representing neuromuscular activities. The nervous system always controls the muscle activity (contraction / relaxation). It's a complex signal, which is controlled by the nervous system and is dependent on the anatomical and physiological properties of muscles. These EMG signal acquires noise while traveling through different tissues. Moreover, the EMG detector, particularly if it is at the surface of the skin, collects signals from different motor units at a time, which may generate interaction of different signals. Due to the complexity of the EMG signal detection of EMG signals with powerful and advance methodologies is becoming a very important requirement in biomedical engineering.

The technology of EMG recording is relatively new. There are still limitations in detection and characterization of existing nonlinearities in the surface electromyography (SEMG) signal, like estimation of the phase, acquiring exact information due to derivation from normality, etc. Traditional system reconstruction algorithms have various limitations and considerable computational complexity and many show high variance [2].

Recent advances in technologies of signal processing and mathematical models have made it practical to develop advanced EMG detection and analysis techniques. Various mathematical techniques and Artificial Intelligence (AI) have received extensive attraction. Mathematical models include time-frequency approaches, Fourier transform, Wigner-Ville Distribution (WVD), statistical measures and higher-order statistics.

AI approaches toward signal recognition include Artificial Neural Networks (ANN), dynamic recurrent neural networks (DRNN) and fuzzy logic system [3]. Genetic Algorithm (GA) has also been applied in evolvable hardware chip for the mapping of EMG inputs to desired hand actions. The electromyography (EMG) signal provides information about the performance of muscles and nerves. At any instant, the shape of the muscle signal, motor unit action potential, is constant unless there is movement of the position of the electrode or biochemical changes in the muscle due to changes in contraction level. The rate of neuron pulses, whose exact times of occurrence are random in nature, is related to the time duration and force of a muscle contraction [4].

In the present research work, the main emphasis is given to pick up SEMG signal and analysis for its application to discriminate motions at different acupressure points, pattern recognition techniques for discriminative system.

## 1.1 Artificial Human Arm's Designs

To improve the prosthetic devices, it is useful to understand the basic differences in the existing available devices. There have been improvements in many of the mechanical artificial arms, but none of them could approach the flexibility of the human arm. A short review of the existing approaches to artificial arm design shows the progress in this field. As a matter of fact, some of the latest approaches, the possibility has been opened for arriving at a much higher degree of perfection than just imitating a few basic human arm movements.

## 1.2 History of Prosthetic Arms

The history of prosthetic arms and hands is a long one, with evidence extending back before Roman times. In 218 BC, in the course of the Second Punic War, the Roman general Marcus sergius had his left hand amputated, but following the fitting of an iron replacement

fashioned to hold his shield, he was able to return to battle. In medieval times, knights would have prosthetic hands made by their armourers. The latter employed the same techniques, so the hands resemble armored gloves. Over the centuries, the pace of development has been limited not only by technological progress, but also by the small number of people who actually survived the trauma of the amputation and the subsequent risk of infection.

## 1.3 Design Classifications of Prosthetic Arms

Prosthetic arm can be classified depending upon its use or controlling techniques. As technology progresses and the number of prosthetic options for individuals with limb deficiencies grow. The two most common prosthetic systems are body-powered and myoelectric designs.

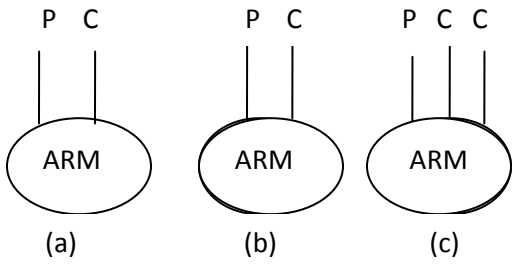


**Fig. 1: (a) Symbolic representation of conventional prosthesis (internally powered and controlled (b) Symbolic representation of externally powered prosthesis. (c) Symbolic representation of prosthesis externally powered and both externally and internally controlled.**

Fig.1 shows different architecture of artificial arm. Here P represents Power Input and C represents Controlling Input**.** A body-powered prosthesis is operated by a harness and cable system designed to capture specific body movement to operate the arm, hook or elbow unit. A myo-electrically-controlled prosthesis uses electrical impulses, generated by contraction of the amputee's own remaining muscles, to operate a motor in a mechanical arm, work hook or elbow. There are many advantages and disadvantages to each type of prosthetic system.

## 1.4 Body-Powered Designs

Body-powered terminal devices come in various configurations. Voluntary opening devices are controlled by the user's pull on the control cable to open the hand or hook, and the grip strength is limited by the number of rubber bands on the hook or the spring tension in the hand. The active grip strength is usually lower in these voluntary opening systems.

Voluntary closing devices provide greater grip strength by closing on the object when the user pulls the control cable. Limitations are found in the inability of the user to maintain the grip strength needed to hold an object for long periods of time or while attempting to manipulate the object in space.

In almost all cases the harness and cable system can be both the best and worst aspect of a body-powered system. Negative aspects develop as the same pressure may create discomfort and contribute to long-term nerve compression and overuse problems.

Another important consideration is that body-powered designs are less expensive for both initial purchase and maintenance relative to myoelectric systems. Primary limitations include restrictive harnessing, poor cosmesis and limited functional grip strength.

## 1.5 Myoelectric Designs

Myoelectric control is the most common type of externally-powered systems, operated by the user's contraction of residual muscle. Most myoelectric systems provide proportional control of the speed and grip strength of the hand or other electric terminal devices (electric hook or work device) based on the strength of the muscle contraction of the wearer.

Many artificial arms include myoelectric hands and passive elbows. Myoelectric elbows can profitably substitute the passive ones only if they can guarantee: durability, low noise, adequate torque, low power consumption, low weight, easy motion control and natural movements. Most of these objectives can be reached by good mechanical design of the

system. Mechanical efficiency of the mechanism is one of the key factors and can be achieved only avoiding long chains of gears [5].

Electrodes are placed on the corresponding sides of the arm that previously performed the desired function. Myoelectric signals are detected by placing three electrodes on the skin. Two electrodes are positioned so there is a voltage between them when a myoelectric signal occurs. The third electrode is placed in a neutral area, and its output is used to cancel the noise that can otherwise interfere with the signals from the other two electrodes. Another important feature of modern myoelectric systems is the interchangeable terminal device.

SEMG was recorded using surface electrodes with the distance between the two active electrodes were maintained while the distant electrode position was fixed for all the experiments. It has been observed that at low levels of muscle contraction there was no significant variation due to the change in the distance between the electrodes. There was a significant change in the amplitude of the SEMG measured by the continuous RMS of the signal. The study has confirmed the well known belief that there **is** an increase in the RMS of SEMG with muscle contraction but the clearly demonstrates that comparison should only be done if the distance between the electrodes is kept constant [6].

For example, a wearer can use an electric arm for everyday activities and situations when cosmesis is important and change to an electric hook or work type device when performing manual labor. This allows multiple gripping options with just a quick change of the terminal device.

The biggest disadvantages to myoelectric systems are cost and system weight. In general, myoelectric systems provide the user with a cosmetically enhanced prosthesis with increased functional grip strength. By reducing or eliminating the harness, the user has the ability to use the prosthesis in more functional positions with greater comfort.

# 2.LITERATURE SURVEY

**Lars H. Lindstrom** [7], Electromyography is the art of describing myoelectric signals. These signals are the electric manifestation of the excitation process preceding the mechanical contraction in muscles. The myoelectric signal, observed with surface electrodes or coaxial needle electrodes, is composed of so-called action potentials originating from the individual muscle fibers. The fibers of the muscle are functionally organized in subgroups, so-called motor units. The activity of each unit is controlled by a motoneuron located in the spinal cord with its axon extending to the muscle.

**Foster B. Stulen** [8], during a sustained muscle contraction, the spectrum of the myoelectric signal is known to undergo compression as a function of time. Previous investigators have shown that the frequency compression is related to the decreasing conduction velocity of the muscle fibers. It is proposed that the frequency compression may be tracked by obtaining a continuous estimate of a characteristic frequency of the spectrum, such as the mean and median, or the ratio of low-frequency components to high-frequency components of the spectrum. A theoretical analysis was performed to investigate the restrictions in estimating the three parameters, as well as their sensitivity to the conduction velocity. A technique is described which determines an unbiased consistent estimate of the median frequency.

**David T. Gibbons** [9], the use of EMG signals from residual muscles to control above-elbow prosthesis has been tried, but presents many problems, not the least being that the prosthesis is under open-loop control. A more satisfactory control technique is extended physiological proprioception where the inherent proprioceptive feedback present within an intact joint is used to provide closed-loop control. Our technique is to control the positioning of this above elbow prosthesis using the motion of the intact shoulder. Grasp, which does not involve positioning in space is separately controlled using EMG signals from biceps and triceps muscles. A choice from a range of linkages can enable the user to perform different tasks in different situations.

**Edward A. Clancy** [10], temporal whitening of individual surface electromyography waveforms and spatial combination of multiple recording sites has separately been demonstrated to improve the performance of EMG amplitude estimation. This investigation combined these two techniques by first whitening, then combining the data from multiple EMG recording sites to form an EMG amplitude estimate. A phenomenological mathematical model of multiple sites of the surface EMG waveform, with analytic solution for an optimal amplitude estimate, is presented. Experimental surface EMG waveforms were then sampled from multiple sites during non fatiguing, constant-force, isometric contractions of the biceps or triceps muscles.

**R. Merletti** [11], the reproducibility of surface myoelectric signal measurements is of paramount importance for clinical applications of electromyography (EMG) techniques. The repeatability of electrically-evoked myoelectric signal shape as well as spectral and amplitude parameters, conduction velocity and elicited torque were tested, in isometric conditions. Contractions were elicited by stimulation of the main muscle motor point and repeated after removal and replacement of the stimulation and detection electrodes in the same carefully marked locations. This protocol was repeated five times on each subject on five different days.

**Paolo Bonato** [12]**,** when the signal is recorded during isometric and constant-force contractions, the spectral scaling towards the lower frequencies mainly results from a progressive reduction of muscle-fiber conduction velocity and from variations of the spatial distribution of depolarization along the muscle fibers. Both phenomena are principally related to the progressive decrement of the interstitial fluid pH, caused by the accumulation of catabolites produced during the contraction.

**P. D'Alessio** [13]**,** the aim of this work is to present an original double-threshold detector of muscle activation, specifically developed for gait analysis. This detector operates on the raw myoelectric signal and, hence, it does not require any envelope detection. Its performances are fixed by the values of three parameters, namely, false-alarm probability, detection

probability and time resolution. Double-threshold detectors are preferable to single-threshold ones because, for a fixed value they yield higher detection probability; furthermore, they allow the user to select the couple false alarm-detection probability with a higher degree of freedom, thus, adapting the performances of the detector to the characteristics of the myoelectric signal of interest and of the experimental situation.

**Z. Escudero** [14], it is proposed the design of a myoelectric prosthesis with two active and one passive degrees of freedom to fit on a limb with an above elbow amputation. It will be controlled by myoelectric electrodes implanted directly on the muscle surface. A person that has undergone by an amputation has lost not only the physical structures of his arm, but also an important part of the system that controlled the amputated limb.

**C. P. Fermo** [15], this work presents the development of a sensor for detecting human muscle contraction, which captures myoelectric signals (EMG), in order to control a myoelectric prosthesis of superior limb. It is proposed a strategy for controlling the artificial hand, based on the myoelectric signal. This way, the patient has a more accurate and easier control of the movement of the prosthetic device, thus leading to a faster adaptation. Through a proposed control strategy, a method to analyze the pattern of the myoelectric signal can be defined. Thus, several kinds of actuating of the artificial hand can be obtained by a simple binary signal or through the analysis of the myoelectric signal pattern.

**Gerhard Staude** [16], various methods to determine the onset of the electromyographic activity which occurs in response to a stimulus has been discussed in the literature over the last decade. Due to the stochastic characteristic of the surface electromyogram (SEMG), onset detection is a challenging task, especially in weak SEMG responses. The performance of the onset detection methods were tested, mostly by comparing their automated onset estimations to the manually determined onsets found by well-trained SEMG examiners. But a systematic comparison between methods, which reveals the benefits and the drawbacks of each method compared to the other ones and show the specific dependence of the detection accuracy on signal parameters, is still lacking.

**S. Venkataramanan** [17], myoelectric control refers to the use of processed Electromyogram (EMG) signals in the operation of devices external to the human body. A variety of myoelectric controller algorithms exist, but there is immense scope for optimization. This paper proposes nu intelligent system which is capable of optimizing the system speed and the number of actions that can be selected. Such as optimization involves rigorous mathematical analysis of the characteristics and the inter-dependence of these two parameters. The intelligent systems employ a technique continuously monitor the actions that are performed. Accordingly, they allocate the least selection duration to those actions that are executed the most number of times.

**Wendy Franks B** [18], a low electrode-electrolyte impedance interface is critical in the design of electrodes for biomedical applications. To design low-impedance interfaces a complete understanding of the physical processes contributing to the impedance is required. In this work a model describing these physical processes is validated and extended to quantify the effect of organic coatings and incubation time. Electrochemical impedance spectroscopy has been used to electrically characterize the interface for various electrode materials.

**Yuet-Ming Lam** [19], this paper presents a methodology that uses surface electromyogram (SEMG) signals recorded from the cheek and chin to synthesize speech. To synthesize a word, SEMG signals recorded during pronouncing a word are blocked into frames; SEMG features are then extracted from each SEMG frame and presented to the neural network to obtain a sequence of speech feature indices. The waveform of the word is then constructed by concatenating the pre-recorded speech segments corresponding to the feature indices. Experimental evaluations based on the synthesis of eight words show that on average over seventy percent of the words can be synthesized correctly.

**Mahdi Khezri** [20], Electromyogram signal (EMG) is an electrical manifestation of contractions of muscles. Surface EMG signal collected form surface of the skin has been used in diverse applications. One of its usages is exploiting it in a pattern recognition system

which evaluates and synthesizes hand prosthesis movements. The ability of current prosthesis has been limited in simple opening and closing that decreases the efficacy of these devices in contrary to natural hand. In order to extend the ability and accuracy of prosthesis arm movements and performance, a novel approach for SEMG pattern recognizing system is proposed.

**M. B. I. Reaz** [21], Electromyography (EMG) signals can be used for clinical/biomedical applications, evolvable hardware chip development, and modern human computer interaction. EMG signals acquired from muscles require advanced methods for detection, decomposition, processing, and classification. The purpose of this paper is to illustrate the various methodologies and algorithms for EMG signal analysis to provide efficient and effective ways of understanding the signal and its nature.

**Dapeng Yang** [22], this paper presents how to extract grasp force information besides mode specifications directly from the myoelectric signals. A force sensor is adopted to record the hand's enveloping force when the hand is performing several grasp modes, synchronously with six channels surface electromyography (EMG) which are extracting from the subject's forearm. Three pattern regression methods, locally weighted projection regression, artificial neural network and support vector machine are used to find the best representative relationship of these two kinds of signals. Experimental results show that the support vector machine method is better, especially in the case of cross-session validation.

**Scott Day** [23], Small electrical currents are generated by muscle fibers prior to the production of muscle force. These currents are generated by the exchange of ions across muscle fiber membranes, a part of the signaling process for the muscle fibers to contract. The signal called the electromyogram (EMG) can be measured by applying conductive elements or electrodes to the skin surface, or invasively within the muscle. Measurement of surface EMG is dependent on a number of factors and the amplitude of the surface EMG signal (SEMG) varies from the uV to the low mV range.

**Yutaro Kobayashi** [24], Electromyographic (EMG) signals have been used to control active prosthetic arms for amputees. One of the obstacles in making such prosthetic arms is the timed estimation of posture, because EMG signals and muscle movements are not necessarily synchronized. It estimated the finger motions for trumpet players by using both surface EMG and the timing information using body motion. The algorithms consisted of Principal Component Analysis and Support Vector Machine. The results showed that applying the timing information using body motion increases how precisely the motion of the fingers is estimated.

**Hardeep S. Ryait** [25], Surface electromyogram (SEMG) is a common method of measurement of muscle activity. It is noninvasive and is measured with minimal risk to the subject. The analysis of SEMG signal depends on a number of factors, such as amplitude as well as time- and frequency-domain properties. The study of SEMG signals at different below elbow muscles for four operations of the hand wrist/grip. Myoelectric signals were extracted by using a single-channel SEMG amplifier consisting of a differential amplifier, non inverting amplifier and interface module. Matlab soft scope was used to acquire the SEMG signal from the hardware. After acquiring the data from six selected locations, interpretations were made for the estimation of parameters of the SEMG using the Matlab-filter algorithm and the fast Fourier transform technique.

**Irena Orovi´c** [26], this paper presents an open-source virtual instrument for time-frequency analysis. The purpose is to show the correct practical implementation, and the performance, of a number of complex algorithms and of a practical criterion (the concentration measure) to select the proper algorithm for a given signal. The virtual instrument provides efficient solutions for signals with a highly non stationary instantaneous frequency. Despite variations of signal phase function, a high concentration can be achieved by a suitable choice of distribution form. A variety of options provides different comparisons for several distributions simultaneously.

# 3.MATERIALS AND METHODS

This chapter describes the electrodes, electrodes theory, acupressure points and finally the Labview used for the analysis of SEMG. SEMG exhibit complex behavior with different complexities. It is a very complex signal which is affected by various factor like anatomical and physiological properties of the muscles.

In the present research work, SEMG was picked up with the help of active electrodes and analyzed with Labview at two acupressure points between elbow and shoulder for four movements at different forces.

## 3.1 Electrodes

To observe the measurement of electro-myo-gram (EMG), a conclusion could easily be reached that the measurement electrodes are simply electrical terminals or contact points from which voltages can be obtained at the surface of the body. Also, the purpose of the electrolyte paste or jelly often used in such measurement might be assumed to be only skin impedance of the system.

These conclusions, however, are incorrect and do not satisfy the theory that explains the origin of bioelectric potentials. It must be realized that the bioelectric potential generated in the body are ionic potentials, produced by ionic current flow. Efficient measurement of these ionic potentials can be measured by conventional methods. It was the realization of this fact that led to the development of the modern noise free, stable measuring devices now available. Devices that convert ionic potential into electronic potentials are called electrodes. The theory of electrodes and principal that govern their design are inherent in an understanding of the measurement of bioelectric potentials.

### 3.1.1 Electrode Theory

The interface of metallic ion in solution with their associated metals results in an electrical potential that is called electrode potential. This potential is a result of the difference in diffusion rate of ions into and out of metal. Equilibrium is produced by the formation of a layer of charge at interface. This charge is really a double layer, with the layer of the metal being one polarity. Non metallic materials, such as hydrogen, also have electrode potential when interfaced with their associated ions in the solution. It is impossible to determine the absolute electrode potential of a single electrode for measurement of potential across the electrode and its ionic solution would require placing another metallic interface in the solution.

All electrode potentials are given as relative values and must be stated in terms of some references. By international agreement the normal hydrogen electrode was chosen as a standard reference and arbitrary assigned an electrode potential of zero volt.

### 3.1.2 Bio Potential Electrodes

A wide variety of electrodes can be used to measure bioelectric potential, but mainly classified into three basic types: microelectrodes, skin surface electrodes and needle electrodes.

All three types of bio potential electrodes have the metal electrolyte interface, in each case, an electrode potential is developed across the interface, proportional to the exchange of ions between the metals and the electrolytes of the body.

The chemical activities that take place within an electrode can cause voltage fluctuations to appear within any physiological input. Such variation may appear as noise on a bioelectric signal. The noise can be reduced by proper choice of materials or, in most cases, by special treatment, such as coating the electrodes by some electrolytic methods to improve stability. It

has been found that a silver-silver chloride electrode is very stable. This type of electrode is prepared by electrolytically coating a piece of pure silver with silver chloride. The coating is normally done by placing a cleaned piece of silver into a bromide free sodium chloride solution. A second piece of silver is also placed in the solution, and the two are connected to a voltage source such that the electrode to be chloride is made positive with respect to each other. The silver ions combine with the chloride ions from the salt to produce neutral silver chloride molecules that coat the silver electrode.

### 3.1.3 Body surface electrodes

Electrodes used to obtain bioelectric potential from the surface of the body are found in many sizes and forms. Although can be used to sense EMG potentials.

**Disposable electrodes**, they eliminate the requirement for cleaning and care after each use. In general, disposable are of floating type with simple snap connectors by which the leads, which are reusable, are attached. Although some disposable electrodes can be reused several times, their cost is usually low enough that for reuse is not warranted. They come pregelled, ready for immediate use.

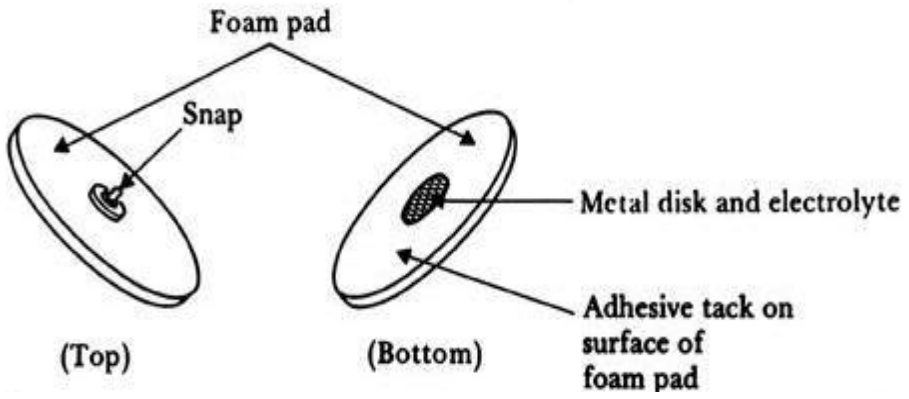


Fig. 3.1 Disposable electrodes

**Active electrodes**, in most EMG readings passive electrodes are used. They are cheap, easy to manufacture and maintenance. They require however special skin preparation in the spot under electrode, and special pastes are also required to lower impedance between electrodes and skin. Those requirements are usually acceptable, but not always welcome.

In present study, active electrodes were used. Active electrode is an electrode that requires no skin preparation. It is possible with preamplifier placed very close to skin (inside the electrode). High dry skin impedance can be omitted by using amplifier with very high input impedance. Another reason to use active electrodes is safety. Because the dry skin-electrode impedance is very high (a few mega ohms) then the isolation barrier is much higher and a chance for an electrocution is much smaller comparing to passive electrodes.

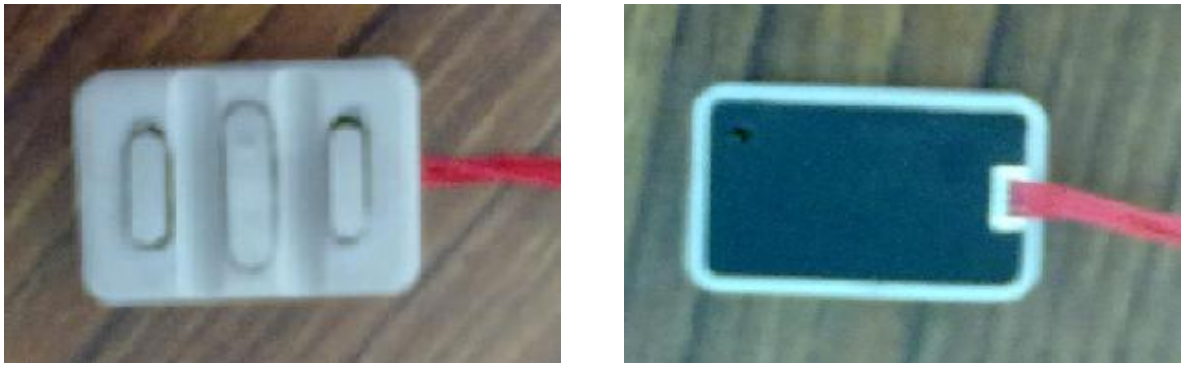

Front view Back view

Fig. 3.2 Active electrode

By integrating the first amplifier stage with a sintered Ag/AgCl electrode, extremely low-noise measurements free of interference are now possible without any skin preparation. The active electrode is a sensor with very low output impedance, so all problems with regards to capacitive coupling between the cable and sources of interference, as well as any artifacts by cable and connector movements are completely eliminated.

Electrodes were placed at acupressure points to pick up the signals.

## 3.2 Acupressure points

Acupressure is a traditional healing practice that involves the application of finger pressure to specific acupuncture points on the body. Pressure on the points is thought to promote circulation, ease muscle tension, and stimulate the body's inherent healing ability. It may help some people who have arm tension and aches from prolonged keyboarding, writing, or any other repetitive movement.

There are several types of pressure points - each is applied differently and each creates a different effect. "Pain points", for example, use tendons, ligaments, and muscles - the goal to temporarily immobilize the target, or at the very least to distract them. Reflex points produce involuntary movements, for example causing the hand to release its grip, the knees to buckle, or the target to gag, or even for the person to be knocked unconscious.

**First Point (P1)**

Fig. 3.3 First acupressure point

Start by bending your arm at about a 45 degree angle. Notice the line that forms in the skin on the inside of the elbow. Press the point at the bottom of the crease on the outside of the arm. You will feel a sharp pain but it will pass quickly. Work the pressure in a circular motion. It is believed that when you press this point you release anger from your body. [27]

**Second Point (P2)**

Fig. 3.4 Second acupressure point

Drop your arm to your side. Use your other hand to find where your shoulder muscle ends and your biceps begin. This will be roughly on the other side of your arm pit on the outside of the arm. Press the point in the middle of your upper arm. The pressure point is believed to help with breathing problems and relieve feelings of sadness. [27]

Once the signal is picked up then send to Labview for analyses purpose.

## 3.3 LabVIEW

LabVIEW is a development system for industrial, experimental, and educational measurement and automation applications based on graphical programming, in contrast to textual programming however, textual programming is supported in LabVIEW. LabVIEW has a large number of functions for numerical analysis and design and visualization of data. LabVIEW is a revolutionary graphical development environment with built in functionality for data acquisition, instrument control, measurement analysis, and data presentation. LabVIEW gives the flexibility of a powerful programming language without the complexity of traditional development environments. LabVIEW delivers extensive acquisition, analysis, and presentation capabilities in a single environment, so that one can seamlessly develop a complete on the platform of choice.

LabVIEW gives development environment for measurement control and automation. Unlike general purpose programming languages, LabVIEW provides functionality specifically tailored to the needs of measurements control, and automation applications, accelerating

development process. From built in analysis capabilities to connectivity with a wide variety of I/O, LabVIEW delivers what engineers and scientists need to quickly build test and measurement, data acquisition, embedded control, scientific research and process monitoring systems.

The LabVIEW graphical development environment gives powerful tools to create applications without writing any lines of text based code. With LabVIEW, one can drag and drop pre-built objects to quickly and simply create user interfaces for the application. Then, one can specify system functionality by assembling block diagrams a natural design notation for scientist and engineers.

LabVIEW has tight Integration with thousands of Instruments and Measurement devices and delivered seamless connectivity with measurement hardware, so one can quickly configure and use virtually any measurement device, including everything from standalone instruments to plug-in data acquisition devices, motion controllers, image acquisition systems, and programmable logic controllers (PLCs).

LabVIEW has open connectivity with Other Applications and furthermore, LabVIEW can allow you to connect to other applications and share data through ActiveX, the Web, DLLs, shared libraries, SQL, TCP/IP, XML, OPC, wireless communication and other methods. LabVIEW's open connectivity enables you to create open, flexible applications that can communicate with other applications across your organization. With LabVIEW, one can develop systems that meet even the most demanding performance requirements across a variety of platforms including Windows, Macintosh, UNIX, or real-time systems.

LabVIEW also includes traditional program development tools. You can set breakpoints, animate program execution to see how the program executes, and single-step through the program to make debugging and program development easier.

### 3.3.1 About LabVIEW

LabVIEW programs are called virtual instruments or VIs because their appearance and operation imitate physical instruments such as oscilloscopes and multi meters. Every VI that information or move it to other files or other computers. A VI contains the following three components:

 **Front panel**— serves as the user interface.

 **Block diagram**— Contains the graphical source code that defines the functionality of the VI.

 **Icon and connector pane**— Identifies the VI so that you can use the VI in another VI. A VI within another VI is called a subVI. A subVI corresponds to a subroutine in text-based programming languages. This section overviews the LabVIEW front panel, block diagram, and palettes. It also explains the dataflow model for program execution that LabVIEW follows

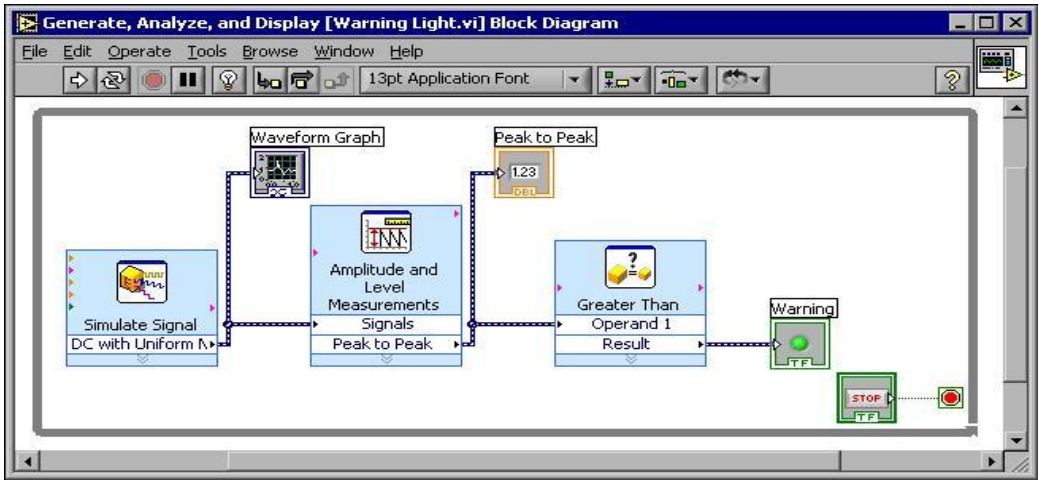


Fig. 3.5 Block diagram

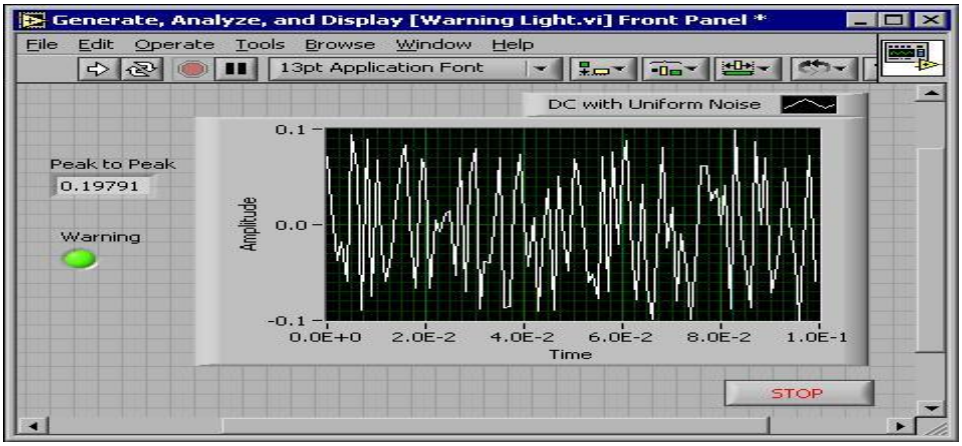


Fig. 3.6 Front panel

### 3.3.2 Data Flow Programming

The programming language used in LabVIEW, also referred to as G, is a dataflow programming language. Execution is determined by the structure of a graphical block diagram (the LV-source code) on which the programmer connects different function nodes by rowing wires. These wires propagate variables and any node can execute as soon as all its input data become available. Since this might be the case for multiple nodes simultaneously, G is inherently capable of parallel execution. Multi-processing and multi-threading hardware is automatically exploited by the built-in scheduler, which multiplexes multiple OS threads over the nodes ready for execution.

### 3.3.3 Graphical Programming

LabVIEW ties the creation of user interfaces (called front panels) into the development cycle. LabVIEW programs/subroutines are called virtual instruments (VIs). Each VI has three components: a block diagram, a front panel, and a connector panel. The last is used to represent the VI in the block diagrams of other, calling VIs. Controls and indicators on the front panel allow an operator to input data into or extract data from a running virtual instrument. However, the front panel can also serve as a programmatic interface. Thus a

virtual instrument can either be run as a program, with the front panel serving as a user interface, or, when dropped as a node onto the block diagram, the front panel defines the inputs and outputs for the given node through the connector pane. This implies each VI can be easily tested before being embedded as a subroutine into a larger program.

The graphical approach also allows non-programmers to build programs simply by dragging and dropping virtual representations of lab equipment with which they are already familiar. The LabVIEW programming environment, with the included examples and the documentation, makes it simple to create small applications. This is a benefit on one side, but there is also a certain danger of underestimating the expertise needed for good quality "G" programming. For complex algorithms or large-scale code, it is important that the programmer possess an extensive knowledge of the special LabVIEW syntax and the topology of its memory management. The most advanced LabVIEW development systems offer the possibility of building stand-alone applications.

The number of advanced mathematic blocks for functions such as integration, filters, and other specialized capabilities usually associated with data capture from hardware sensors is Immense. In addition, LabVIEW includes a text-based programming component called Math Script with additional functionality for signal processing, analysis and mathematics. Math Script can be integrated with graphical programming using "script nodes" and uses a syntax that is generally compatible with MATLAB.

The fully object-oriented character of LabVIEW code allows code reuse without modifications: as long as the data types of input and output are consistent, two sub VIs are interchangeable. The LabVIEW Professional Development System allows creating stand-alone executables and the resultant executable can be distributed an unlimited number of times.

## 3.4 NI-DAQ

Using NI-DAQ, you can easily acquire, analyze, and present your measurements in LabVIEW. Figure 4 shows the block diagram of a typical data acquisition in LabVIEW. With the first set of NI-DAQ VIs, you configure your acquisition and read data from your sensor. Because this VI uses a named channel, most of the signal conditioning and DAQ hardware configuration is handled automatically. Next, you route the waveform from the read VI to the peak detect measurement VI.

The waveform data type carries the scaled sensor and time data to the measurement function. Finally, the measurement data can be displayed in an indicator and/or a waveform graph that automatically has the correct time and engineering units.

The quality of your configuration and driver software is just as important as the quality of your measurement hardware. NI-DAQ is a robust, time-proven driver for NI data acquisition and signal conditioning hardware. This software helps you quickly install your device and begin taking measurement data. NI-DAQ includes hundreds of application examples to jump-start your application development. NI-DAQ delivers the same ease of use and performance across many development environments, operating systems, and computer buses.

NI-DAQ is the robust driver software included with all National Instruments data acquisition and signal conditioning products. This easy-to-use software tightly integrates the full functionality of your DAQ hardware to LabVIEW, Lab Windows/CVI, and Measurement Studio for Visual basic. High-performance features include multi device synchronization, networked measurements, and DMA data management.

Bundled with NI-DAQ, the Measurement & Automation Explorer utility simplifies the configuration of your measurement hardware with device test panels, interactive measurements, and scaled I/O channels. NI-DAQ also provides numerous example programs for LabVIEW and other application development environments to get you started with your application quickly.

NI-DAQ software isolates you from hardware-specific register commands and gives you a simple, yet powerful application programming interface (API) between the complete hardware capabilities and a wide variety of development environments and languages. Because of the consistent API, you can use different DAQ hardware with the same application without modifying your software.

Data Acquisition System (NI-DAQ (PCI-6024E))

| | | | |
|---|---|---|---|
| ACH8 | 34 | 68 | ACH0 |
| ACH1 | 33 | 67 | AIGND |
| AIGND | 32 | 66 | ACH9 |
| ACH10 | 31 | 65 | ACH2 |
| ACH3 | 30 | 64 | AIGND |
| AIGND | 29 | 63 | ACH11 |
| ACH4 | 28 | 62 | AISENSE |
| AIGND | 27 | 61 | ACH12 |
| ACH13 | 26 | 60 | ACH5 |
| ACH6 | 25 | 59 | AIGND |
| AIGND | 24 | 58 | ACH14 |
| ACH15 | 23 | 57 | ACH7 |
| DAC0OUT[1] | 22 | 56 | AIGND |
| DAC1OUT[1] | 21 | 55 | AOGND |
| RESERVED | 20 | 54 | AOGND |
| DIO4 | 19 | 53 | DGND |
| DGND | 18 | 52 | DIO0 |
| DIO1 | 17 | 51 | DIO5 |
| DIO6 | 16 | 50 | DGND |
| DGND | 15 | 49 | DIO2 |
| +5 V | 14 | 48 | DIO7 |
| DGND | 13 | 47 | DIO3 |
| DGND | 12 | 46 | SCANCLK |
| PFI0/TRIG1 | 11 | 45 | EXTSTROBE* |
| PFI1/TRIG2 | 10 | 44 | DGND |
| DGND | 9 | 43 | PFI2/CONVERT* |
| +5 V | 8 | 42 | PFI3/GPCTR1_SOURCE |
| DGND | 7 | 41 | PFI4/GPCTR1_GATE |
| PFI5/UPDATE* | 6 | 40 | GPCTR1_OUT |
| PFI6/WFTRIG | 5 | 39 | DGND |
| DGND | 4 | 38 | PFI7/STARTSCAN |
| PFI9/GPCTR0_GATE | 3 | 37 | PFI8/GPCTR0_SOURCE |
| GPCTR0_OUT | 2 | 36 | DGND |
| FREQ_OUT | 1 | 35 | DGND |

Fig. 3.7 Pin diagram of NI DAQ 6024 E

## 3.5 Force Gripper

In the present work, the SEMG signal was taken from the two selected acupressure points with the help of active electrodes. The signal obtain from the active electrodes is amplified signal and given to software through DAQ card. The SEMG signal taken for the different movements and at the different forces (ww, 10 kg, 20 kg, 30 kg) with the help of gripper. The image of gripper used in my work is given below:

Fig. 3.8 Force gripper

# 4. METHODOLOGY

SEMG signals were recorded from the surface of the body by using active electrodes which include preamplifiers. The ±5 V supply is given to electrodes. These signals were analyzed using Labview. The signal is taken for the different movements at different forces from different objects.

Firstly signal is saved by Labview 6 and then processed using Labview 2009. About 1024 samples were recorded for the time window of 1000ms of the soft scope in the workspace. A program was made to filter the signal from 70 to 250 Hz as band pass filter and then different parameters like $V_{rms}$, standard deviation, power spectrum, maximum frequency components and spectrogram were calculated. Fig. 4.1 shows the block diagram of the system.

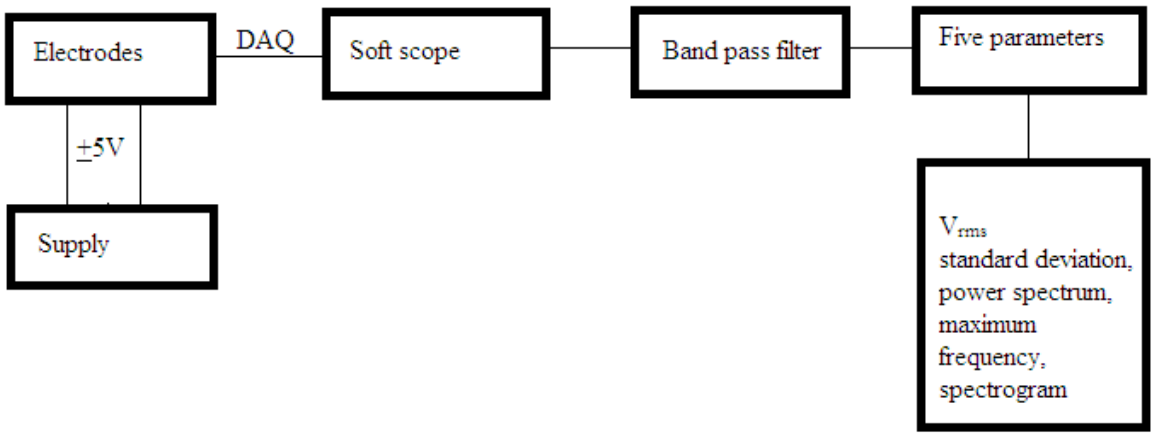


Fig. 4.1 block diagram of the system

Firstly, the signal is saved by the program made in Labview 6. A virtual channel was made at which signal is received which is named as ‘a1’. Then, the signal from this channel is given to ‘daq configure.vi’.

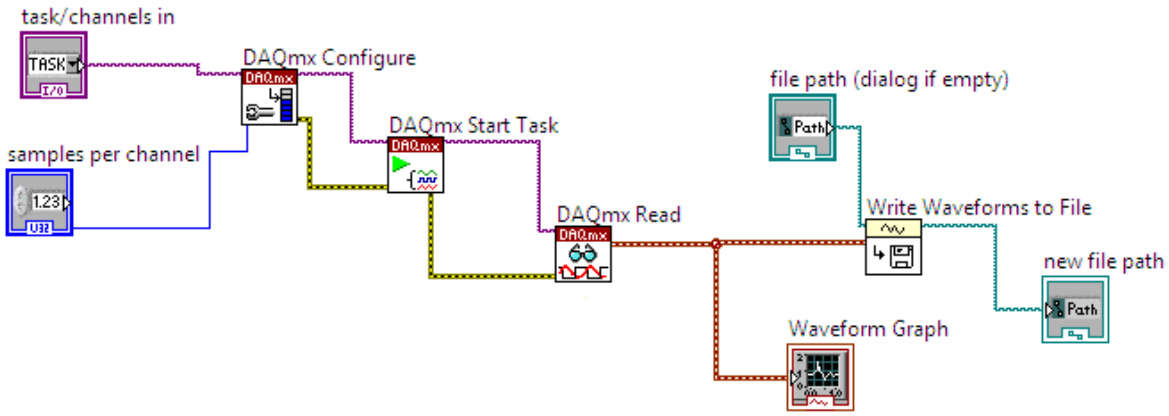


Fig 4.2 (a) Block diagram of program to save data

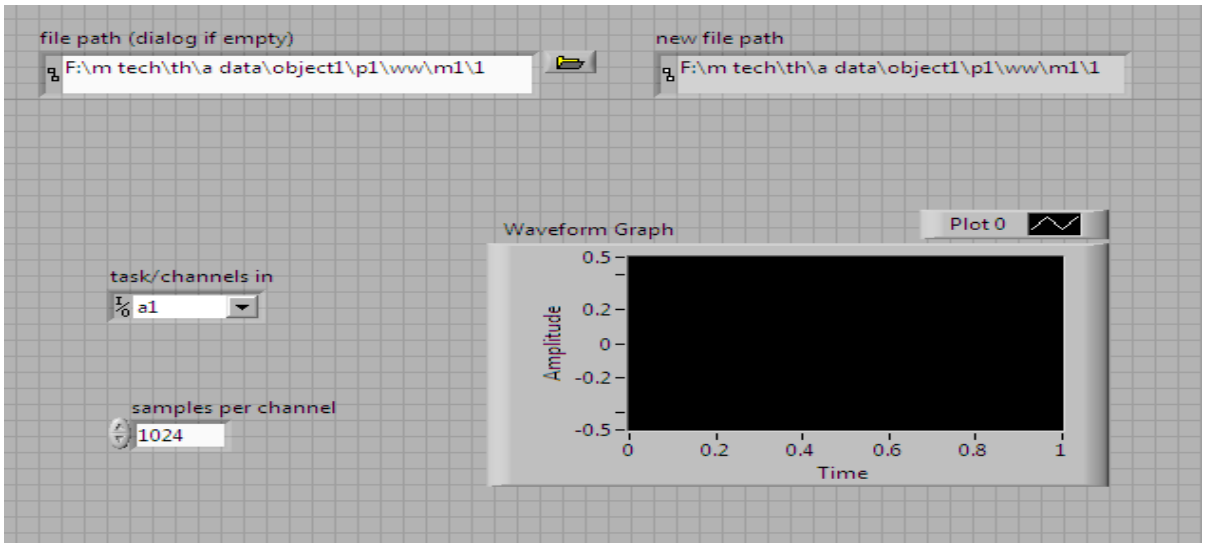


Fig 4.2 (b) Front panel of program to save data

The signal is then given to ‘daq start.vi’ and after that ‘daq read.vi’. This program read the signal from the data acquisition card. Now to save this signal ‘write waveform to file.vi’ was used and the ‘file path’ is the path where it saved the signal. Fig. 4.2 (a) shows the block diagram of the program to save the signal and Fig. 4.2 (b) shows the front panel of the program.

Now this saved signal can be read any time by using this program and any processing can be done on this signal.

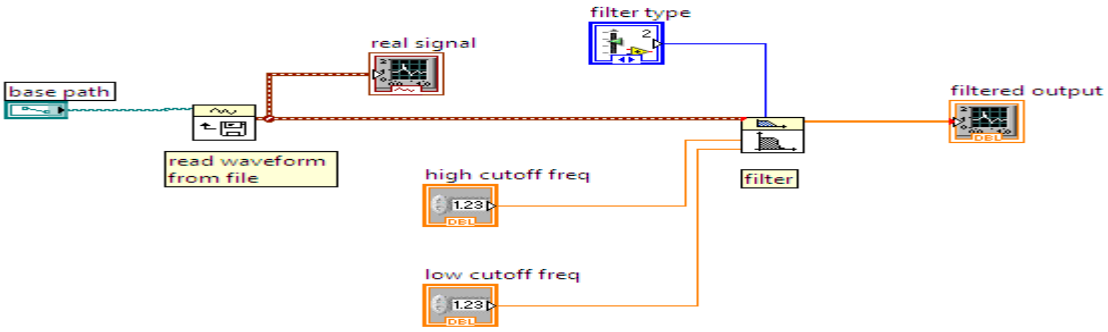


Fig 4.3 (a) Block diagram of program to filter signal

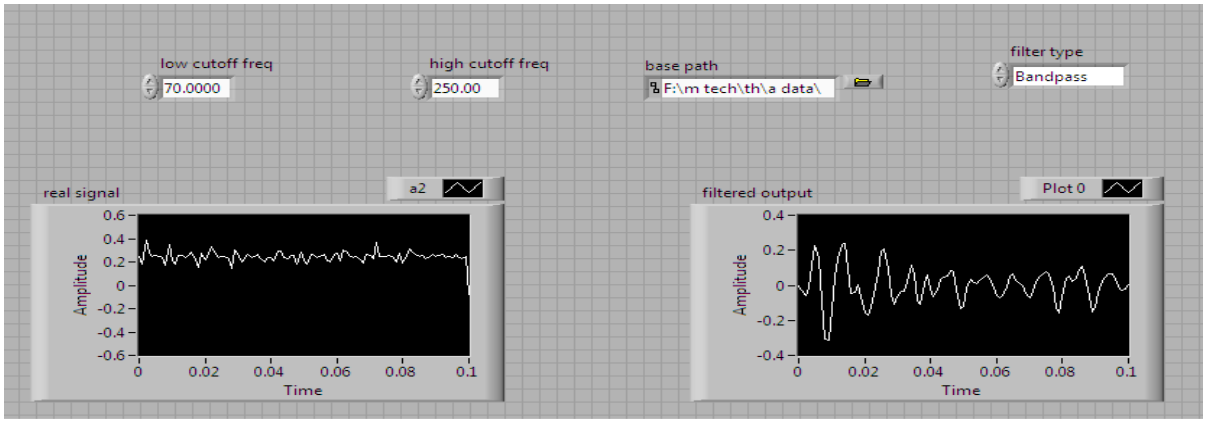


Fig 4.3 (b) Front panel of program to filter signal

In this program, the saved signal is read by using 'read waveform from file.vi'. That gives the waveform in output and then this waveform is filtered by 'filter.vi' that gives 70 to 250 Hz filtered output as band pass filter. The 'real signal' is the saved signal and the 'filtered output' is the filtered output waveform. The low cut of frequency is 70 Hz and high cut of frequency is 250 Hz. Fig 4.3 (a) shows the block diagram of program to filter the saved signal Fig 4.3 (b) shows the front panel of program.

## 4.1 Root mean square value

The root mean square (abbreviated RMS or rms), also known as the quadratic mean, is a statistical measure of the magnitude of a varying quantity. It is especially useful when variants are positive and negative. The RMS value of a set of values (or a continuous-time waveform) is the square root of the arithmetic mean (average) of the squares of the original values (or the square of the function that defines the continuous waveform).

The eq. 1 gives the RMS value for 'n' samples. Fig 4.4 (a) shows the block diagram of program to calculate RMS value. Fig 4.4 (b) shows the front panel of program to calculate RMS value. The RMS value is given by:

$$V_{rms} = \sqrt{\frac{(x_1^2 + x_2^2 + x_3^2 + \ldots\ldots\ldots\ldots\ldots\ldots + x_n^2)}{n}} \qquad (1)$$

where,

$V_{rms}$ – the root mean square value

$X_i$ – value of samples

n- no. of samples

Program to calculate $V_{rms}$:

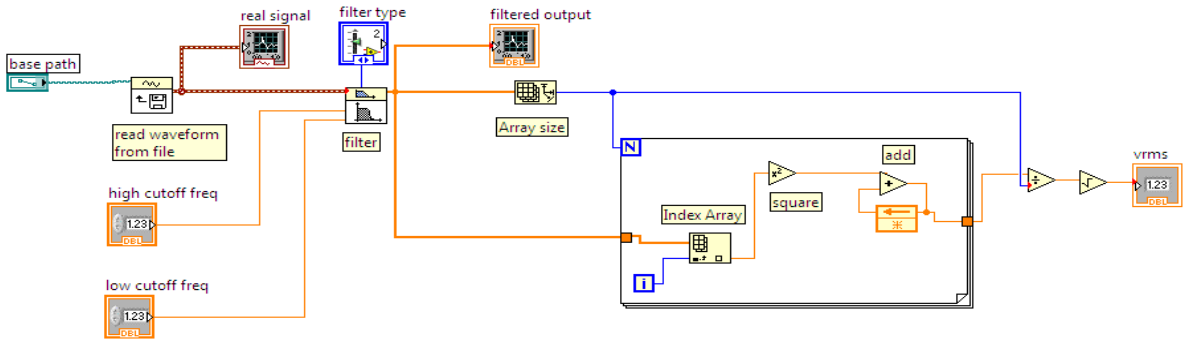


Fig 4.4 (a) Block diagram of program to calculate RMS value

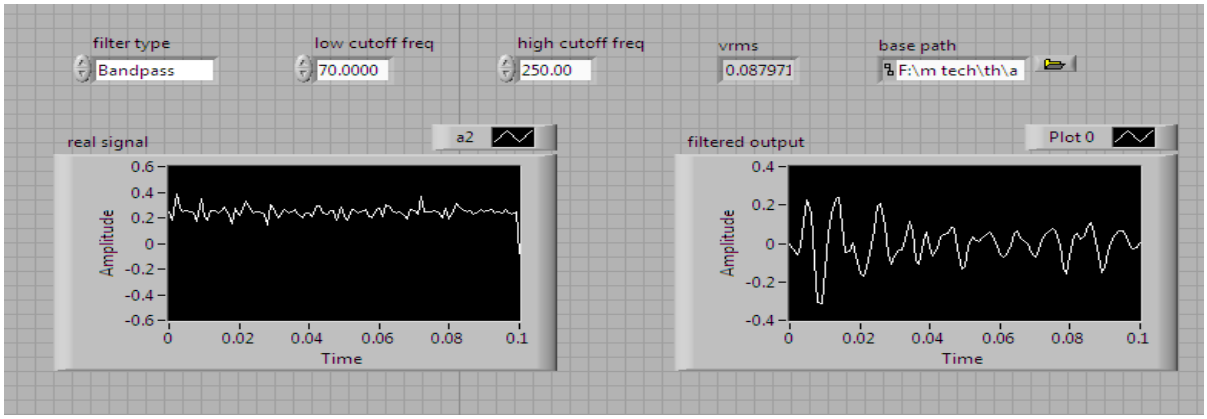


Fig 4.4 (b) Front panel of program to calculate RMS value

## 4.2 Standard Deviation

Standard deviation is widely used measurement of variability or diversity used in statistics and probability theory. It shows variation or dispersion from the average (mean, or expected value). A low standard deviation indicates that the data points tend to be very close to the mean whereas high standard deviation indicates that the data are spread out over a large range of values. Fig 4.5 (a) shows the block diagram of program to calculate standard deviation and Fig 4.5 (b) shows the front panel of program to calculate standard deviation. The standard deviation is given by:

$$SD = \sqrt{\frac{\sum(x_i - u)^2}{n-1}} \quad (2)$$

Where,

SD – standard deviation

$x_i$ - Value of samples

u – mean

n – no. of samples

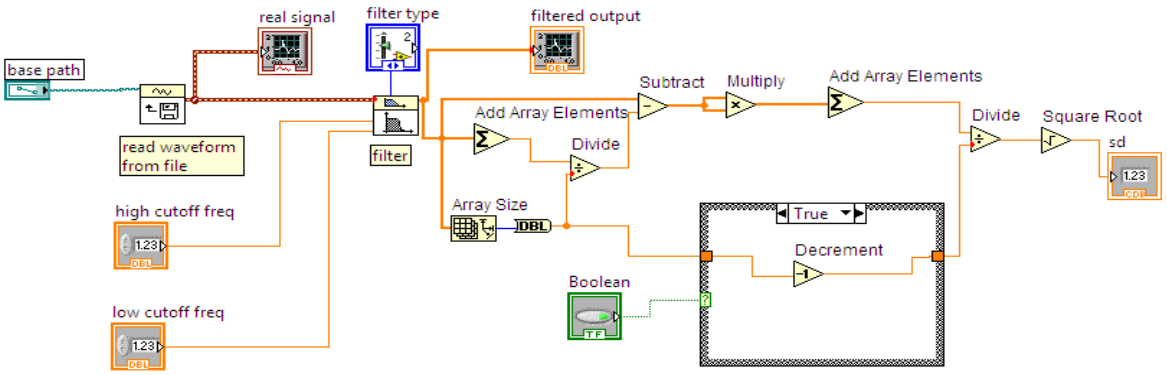


Fig 4.5 (a) Block diagram of program to calculate Standard deviation

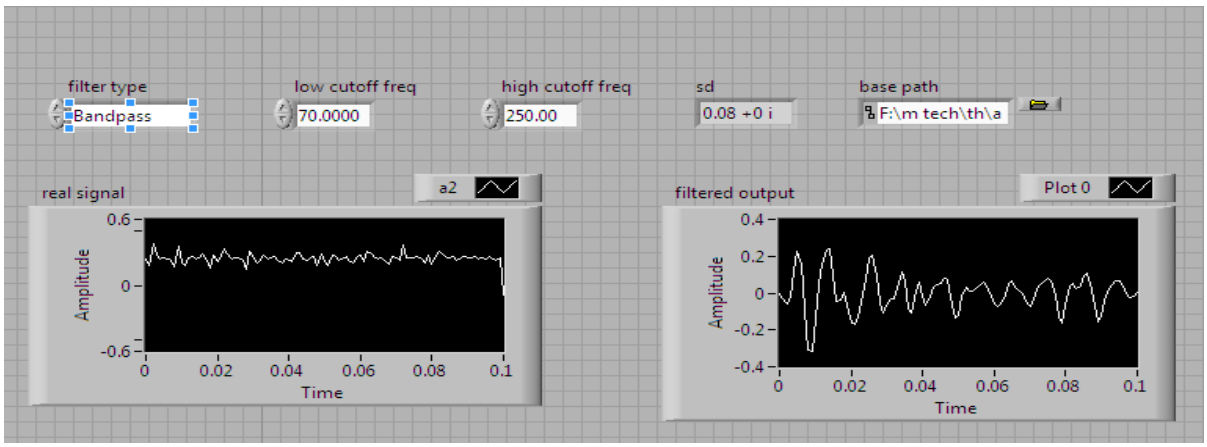


Fig 4.5 (b) Front panel of program to calculate standard deviation

## 4.3 Power Spectrum

Power spectrum gives the signal frequency. Here, periodic signals give peaks at a fundamental and its harmonics; quasi periodic signals give peaks at linear combinations of two or more irrationally related frequencies (often giving the appearance of a main sequence and sidebands); and chaotic dynamics give broad band components to the spectrum. For a given signal, the power spectrum gives a plot of the portion of a signal's power (energy per unit time) falling within given frequency bins. Fig 4.6 (a) shows the block diagram of program for power spectrum and Fig 4.6 (b) shows the front panel of program for power spectrum.

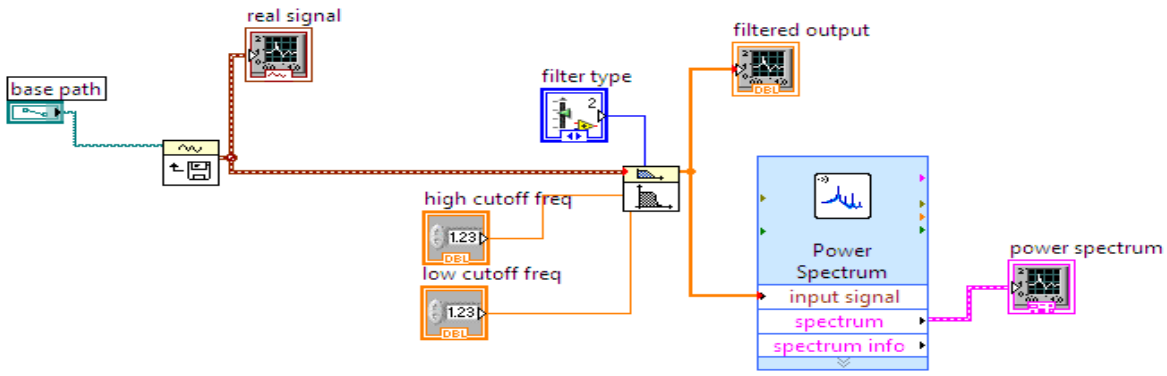


Fig 4.6 (a) Block diagram of program for power spectrum

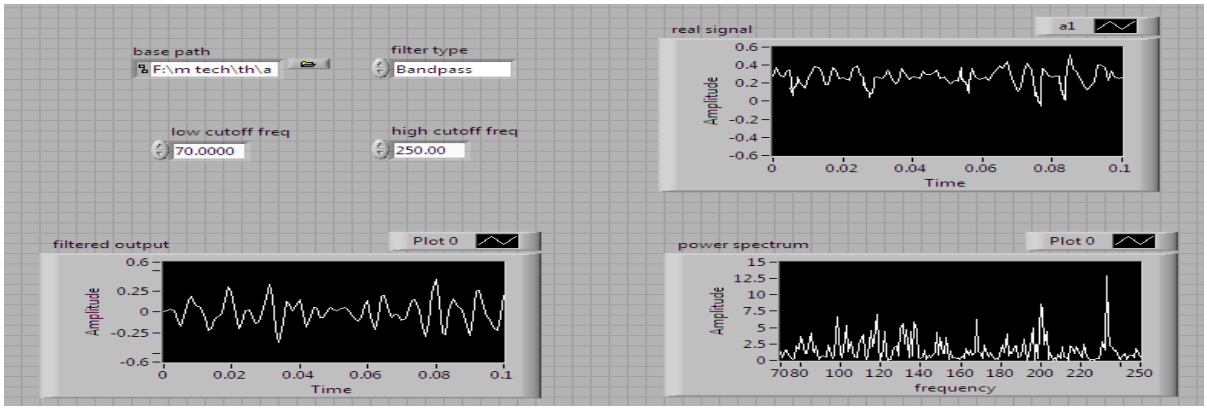


Fig 4.6 (b) Front panel of program for power spectrum

## 4.4 Maximum frequency component

Maximum frequency component is the frequency at which signal has maximum amplitude, i.e. signal is most dominated at that frequency. In the present work, 'peak search.vi' gives the maximum frequency component but its output is an array and each element is a cluster of elements that is frequency and its value. Then break each element of cluster and find maximum amplitude and its frequency by 'max and min.vi'. Fig 4.7 (a) shows the block diagram of program to calculate maximum frequency component and Fig 4.7 (b) shows the front panel of program to calculate maximum frequency component.

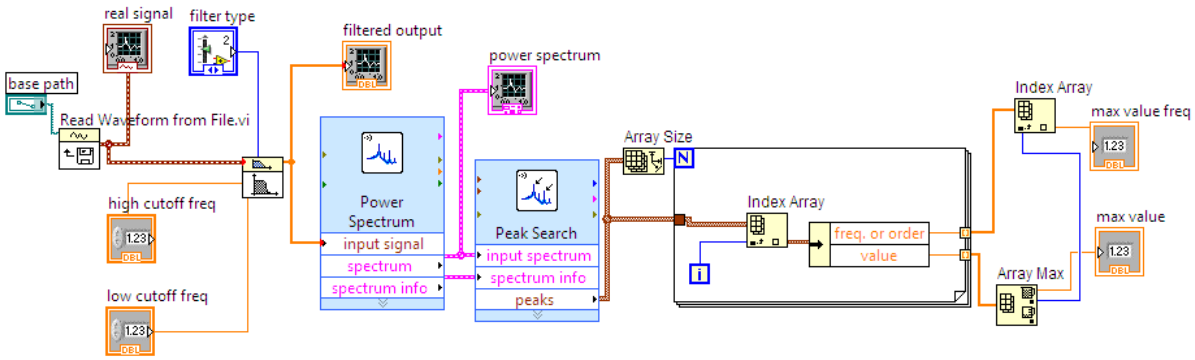


Fig 4.7 (a) Block diagram of program to calculate maximum frequency component

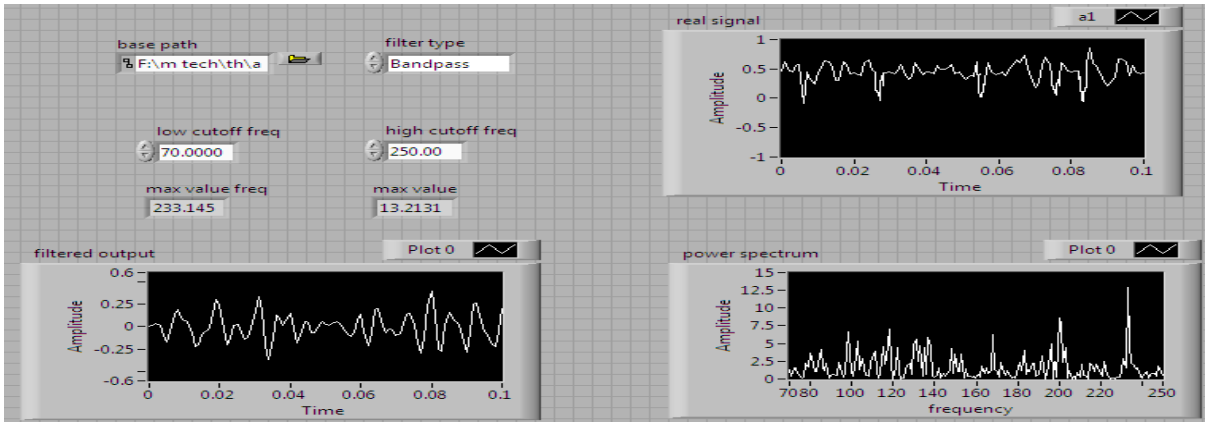


Fig 4.7 (b) Front panel of program to calculate maximum frequency component

## 4.5 Spectrogram and Wigner, Choi Willa distribution

A spectrogram is a time-varying spectral representation that shows spectral density of a signal variation with time. In the field of time–frequency signal processing, it is one of the most popular quadratic Time-Frequency Distribution that represents a signal in a joint time-frequency domain and that has the property of being positive.

Here, the signal waveform gives pressure or amplitude of the signal vs. time. From the waveform one can compute parameters like average level, beginning and end of segments etc.

"Wigner-Ville Distribution (WVD)" (or "Wigner-Ville Spectrum") which is functionally similar to a spectrogram. It gives better temporal and frequency resolution at the expense of many artifacts and introduce negative values which would correspond to negative energy. These are known issues with the W-V spectrum and there are ways to compensate.

The ‘Choi Willa distribution (CWD)’ reduces the cross-terms generated by two auto-terms with different time centers and frequency centers. The Choi Willa distribution has a coarser time-frequency resolution and it also blurs the auto-terms when the Choi Willa distribution reduces the cross-terms.

In other words, the Choi Willa distribution does not suppress the cross-terms that two auto-terms with the same time center or frequency center generate. Fig 4.8 (a) shows the block diagram of program for spectrogram, Wigner and Choi Willa distribution and Fig 4.8 (b) shows the front panel of program for spectrogram, Wigner and Choi Willa distribution

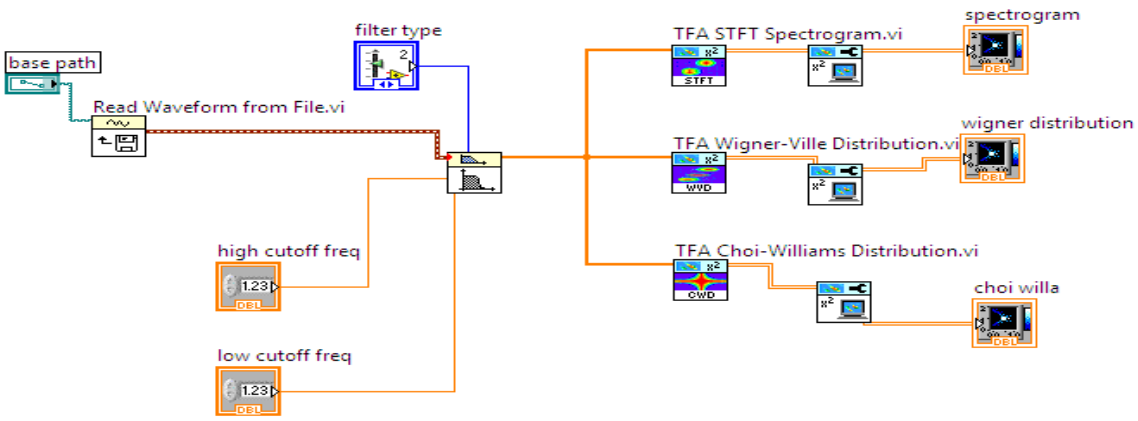


Fig 4.8 (a) Block diagram of program for spectrogram, Wigner and Choi Willa distribution

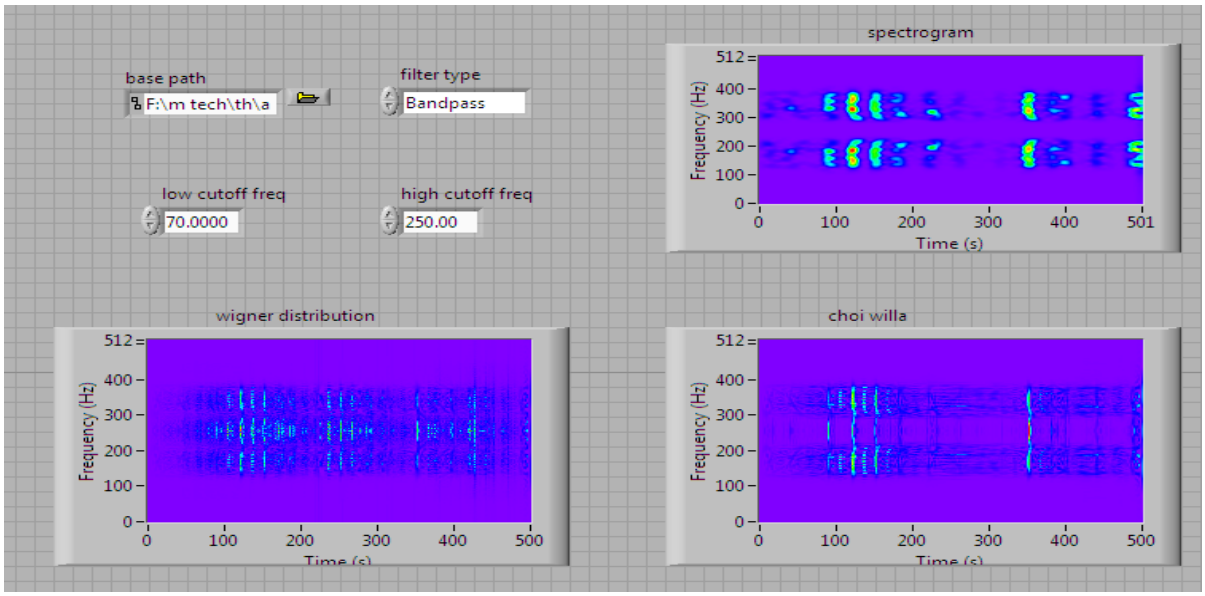


Fig 4.8 (b) Front panel of program for spectrogram, Wigner and Choi Willa distribution

# 5. RESULTS AND DISCUSSION

The observations were taken from the different objects for different movements from the two different points at the different forces and tabulated in tables 5.1 to 5.4. Three observations were taken for the one movement. Firstly, RMS values were calculated for the different observations. Table 5.1 shows the RMS values of one object from first point (P1). Table 5.2 shows the RMS values of one object from second point (P2). Table 5.3 shows the RMS values of second object from first point (P1). Table 5.4 shows the RMS values of second object from second point (P2).

Table 5.1 RMS values of first object from P1

| Force | movements | 1 | 2 | 3 |
|---|---|---|---|---|
| Ww | m1 | 0.114769 | 0.108026 | 0.107988 |
| | m2 | 0.0737 | 0.07272 | 0.071322 |
| | m3 | 0.100124 | 0.09089 | 0.094311 |
| | m4 | 0.082162 | 0.0847 | 0.0778 |
| | | | | |
| 10 | m1 | 0.138502 | 0.119026 | 0.112832 |
| | m2 | 0.082698 | 0.0737 | 0.080969 |
| | m3 | 0.100518 | 0.1065 | 0.098012 |
| | m4 | 0.091959 | 0.08896 | 0.0915 |
| | | | | |
| 20 | m1 | 0.184817 | 0.15233 | 0.153057 |
| | m2 | 0.09979 | 0.10908 | 0.090032 |
| | m3 | 0.146418 | 0.144675 | 0.130625 |
| | m4 | 0.093588 | 0.10792 | 0.087878 |
| | | | | |
| 30 | m1 | 0.218532 | 0.208692 | 0.193092 |
| | m2 | 0.165761 | 0.15233 | 0.163225 |
| | m3 | 0.1875 | 0.19634 | 0.18427 |
| | m4 | 0.175489 | 0.1633 | 0.17143 |

Table 5.2 RMS values of first object from P2

| Force | movements | 1 | 2 | 3 |
|---|---|---|---|---|
| Ww | m1 | 0.087912 | 0.08708 | 0.08478 |
| | m2 | 0.07912 | 0.0708 | 0.07748 |
| | m3 | 0.0719 | 0.0671 | 0.0692 |
| | m4 | 0.051404 | 0.0512 | 0.047993 |
| | | | | |
| 10 | m1 | 0.103211 | 0.10391 | 0.103773 |
| | m2 | 0.096234 | 0.09336 | 0.09136 |
| | m3 | 0.09233 | 0.09263 | 0.09036 |
| | m4 | 0.060149 | 0.059413 | 0.05528 |
| | | | | |
| 20 | m1 | 0.117123 | 0.113457 | 0.113854 |
| | m2 | 0.113082 | 0.1109 | 0.107165 |
| | m3 | 0.0983 | 0.102935 | 0.095004 |
| | m4 | 0.080912 | 0.08108 | 0.07998 |
| | | | | |
| 30 | m1 | 0.164313 | 0.158313 | 0.15513 |
| | m2 | 0.142851 | 0.14082 | 0.1331 |
| | m3 | 0.10898 | 0.1146 | 0.10946 |
| | m4 | 0.098989 | 0.1044 | 0.095389 |

Table 5.3 RMS values of second object from P1

| Force | movements | 1 | 2 | 3 |
|---|---|---|---|---|
| Ww | m1 | 0.091603 | 0.10012 | 0.09211 |
| | m2 | 0.069343 | 0.063241 | 0.072126 |
| | m3 | 0.092713 | 0.0838 | 0.082508 |
| | m4 | 0.0854 | 0.081222 | 0.07941 |
| | | | | |
| 10 | m1 | 0.119215 | 0.11705 | 0.118123 |
| | m2 | 0.0828 | 0.081858 | 0.0751 |
| | m3 | 0.102551 | 0.10815 | 0.102612 |
| | m4 | 0.10091 | 0.1025 | 0.10144 |
| | | | | |
| 20 | m1 | 0.131356 | 0.124581 | 0.127392 |
| | m2 | 0.094173 | 0.0932 | 0.09065 |
| | m3 | 0.121876 | 0.1226 | 0.111496 |
| | m4 | 0.114 | 0.1176 | 0.096974 |
| | | | | |
| 30 | m1 | 0.16615 | 0.17215 | 0.16215 |
| | m2 | 0.111684 | 0.10779 | 0.10643 |
| | m3 | 0.158894 | 0.140094 | 0.15394 |
| | m4 | 0.136559 | 0.13156 | 0.12932 |

Table 5.4 RMS values of second object from P2

| Force | movements | 1 | 2 | 3 |
|---|---|---|---|---|
| Ww | m1 | 0.082188 | 0.074673 | 0.07652 |
| | m2 | 0.055836 | 0.05886 | 0.063856 |
| | m3 | 0.06924 | 0.07 | 0.074387 |
| | m4 | 0.05275 | 0.04621 | 0.052496 |
| | | | | |
| 10 | m1 | 0.0914 | 0.084963 | 0.08963 |
| | m2 | 0.0705 | 0.0725 | 0.067795 |
| | m3 | 0.073156 | 0.06569 | 0.074164 |
| | m4 | 0.057018 | 0.0604 | 0.055684 |
| | | | | |
| 20 | m1 | 0.125043 | 0.128653 | 0.126782 |
| | m2 | 0.116782 | 0.115043 | 0.11083 |
| | m3 | 0.11282 | 0.11043 | 0.10783 |
| | m4 | 0.09411 | 0.08965 | 0.08893 |
| | | | | |
| 30 | m1 | 0.158894 | 0.144354 | 0.141988 |
| | m2 | 0.141923 | 0.141257 | 0.135 |
| | m3 | 0.1297 | 0.1327 | 0.1282 |
| | m4 | 0.10082 | 0.10243 | 0.10783 |

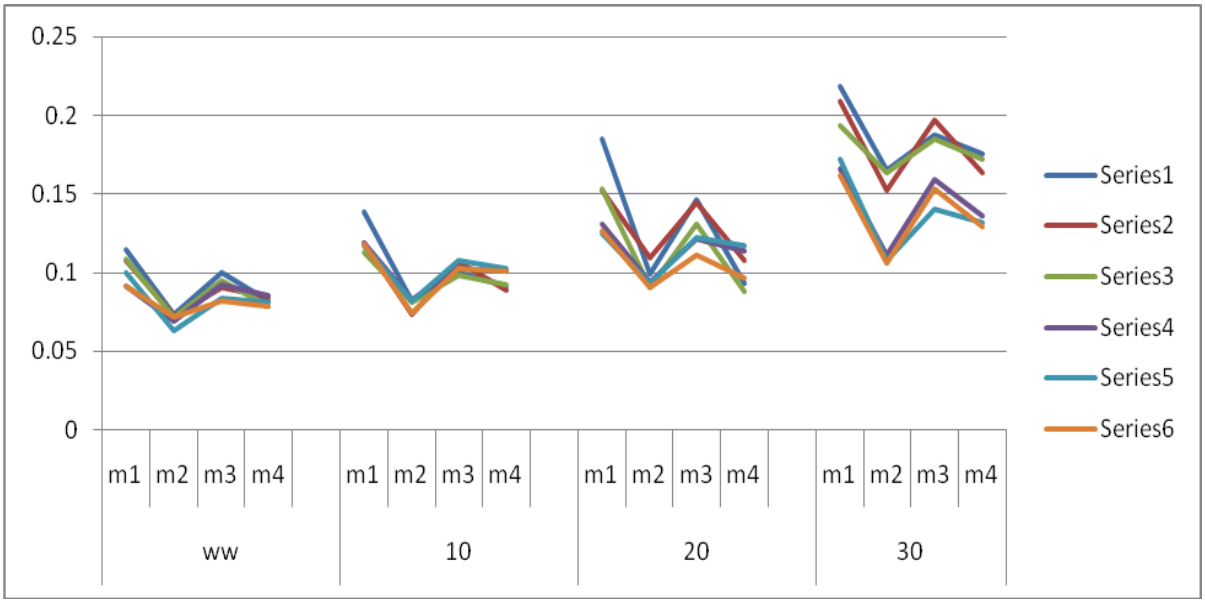


Fig. 5.1 Plot for P1 between RMS values vs different motions at different forces

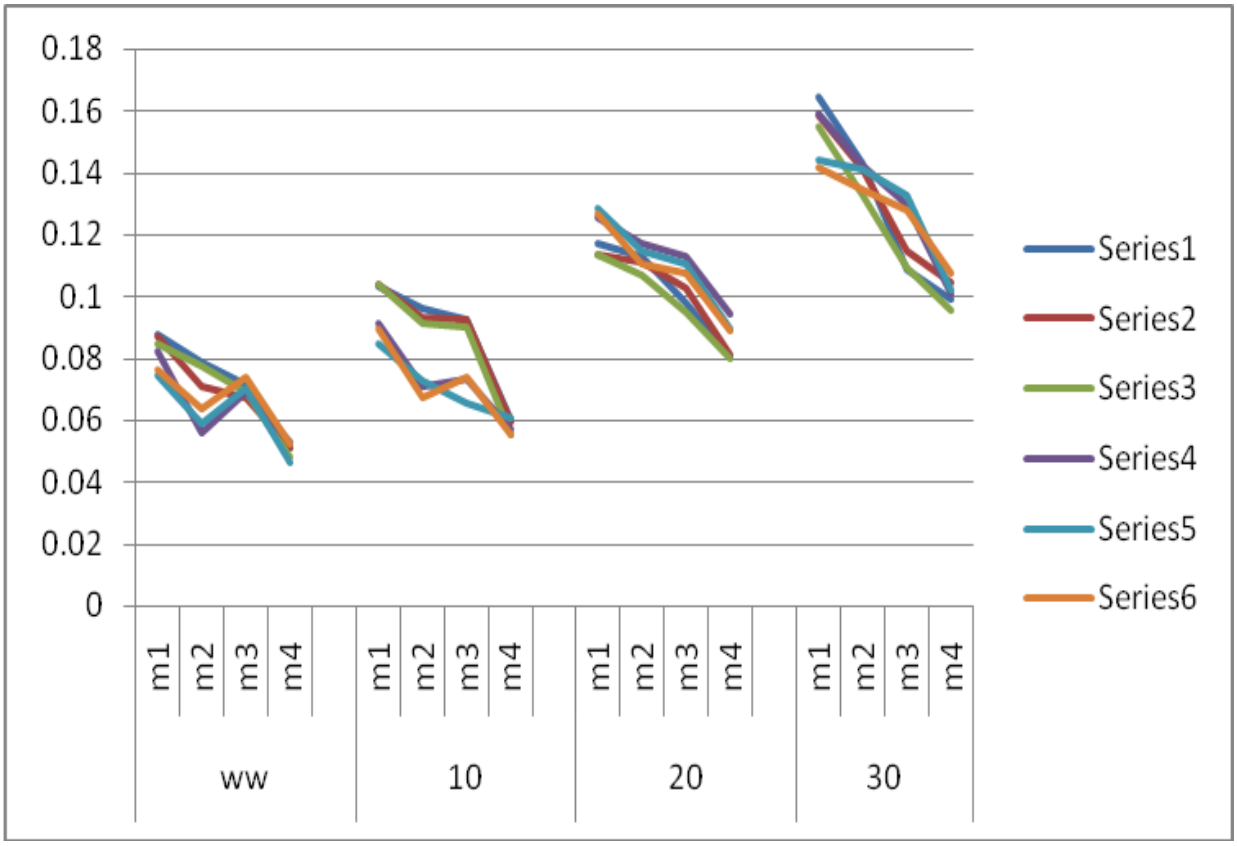


Fig. 5.2 Plot for P2 between rms values vs different motions at different forces

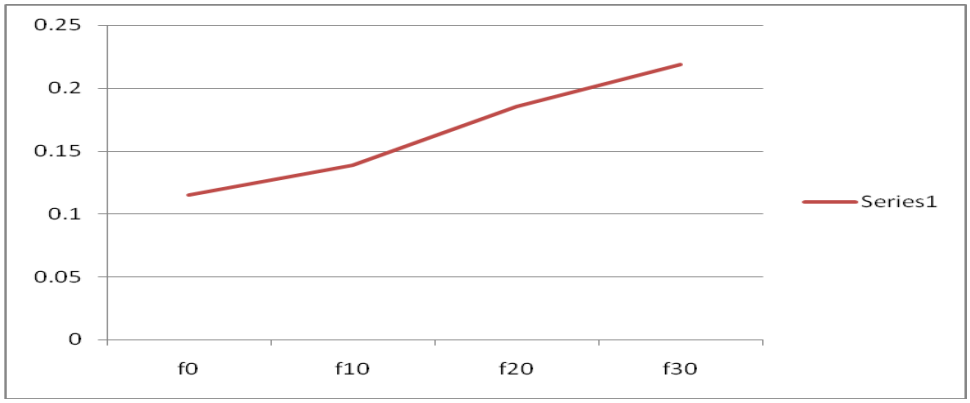


Fig. 5.3 Plot between force vs RMS values

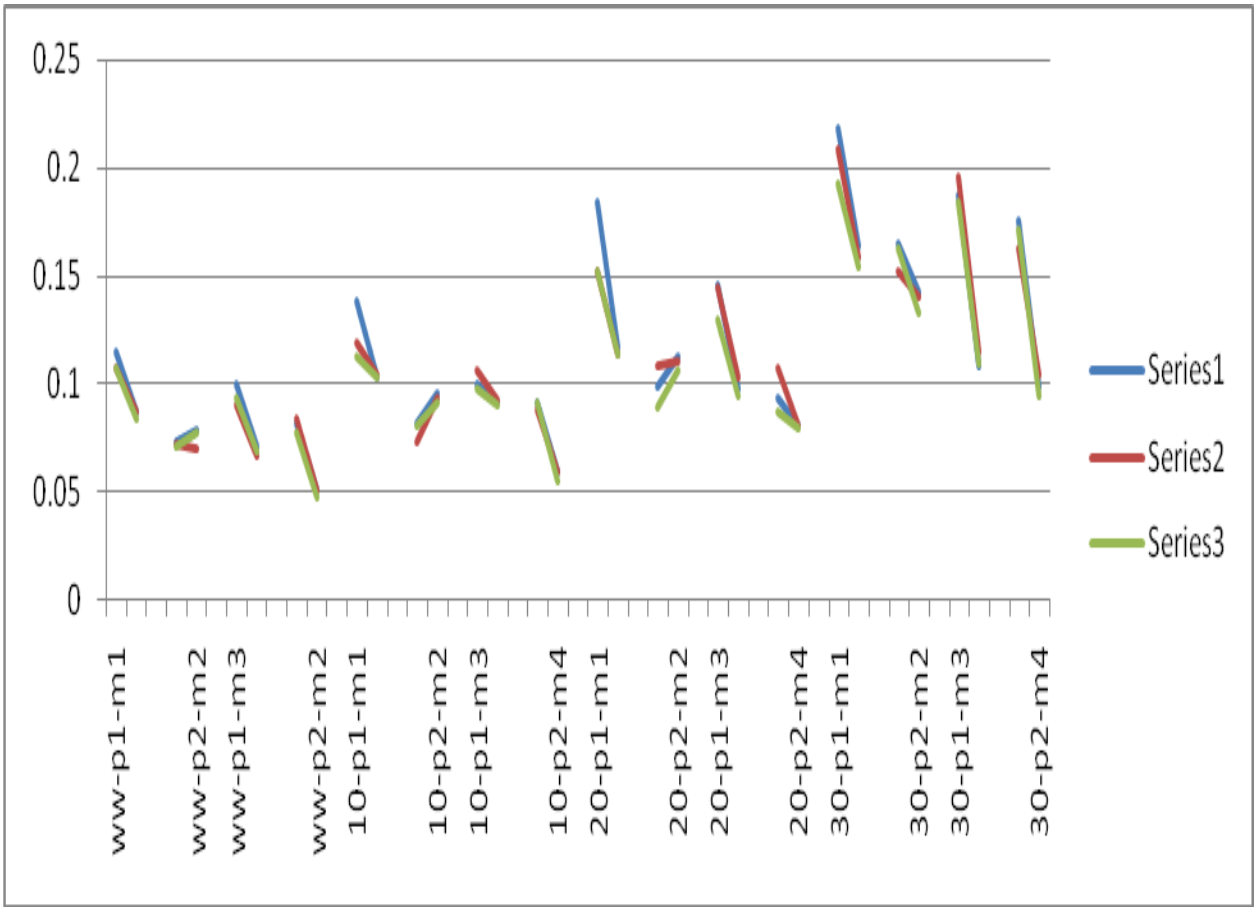


Fig. 5.4 Plot for RMS values for P1 and P2

## 5.1 For RMS values

At different gripping forces, RMS values of the SEMG signals were recorded. Fig. 5.1 shows the variation for 'P1' RMS values and different motions at different forces. It shows that the 'm1' has more RMS value than 'm2' and 'm3' has more RMS value than 'm4'. Fig. 5.2 shows the variation for 'P2' RMS values and different motions at different forces. Fig. 5.3 shows the variation of force and RMS values which remains linear RMS values. Fig. 5.4 shows the variation for RMS values for P1 and P2. It shows that that P1 has more RMS values as compared to 'P2'. It means 'P1' is more dominating point.

Table 5.5 shows the standard deviation of one object from first point (P1). Table 5.6 shows the standard deviation of one object from second point (P2). Table 5.7 shows the standard deviation of second object from first point (P1). Table 5.8 shows the standard deviation of second object from second point (P2).

Table 5.5 standard deviation of first object from P1

| force | movement | 1 | 2 | 3 |
|---|---|---|---|---|
| ww | m1 | 0.11 | 0.1 | 0.1 |
| | m2 | 0.07 | 0.07 | 0.07 |
| | m3 | 0.1 | 0.09 | 0.09 |
| | m4 | 0.08 | 0.08 | 0.07 |
| 10 | m1 | 0.13 | 0.11 | 0.11 |
| | m2 | 0.08 | 0.07 | 0.08 |
| | m3 | 0.1 | 0.1 | 0.09 |
| | m4 | 0.09 | 0.08 | 0.09 |
| 20 | m1 | 0.18 | 0.15 | 0.15 |
| | m2 | 0.09 | 0.1 | 0.09 |
| | m3 | 0.14 | 0.14 | 0.13 |
| | m4 | 0.09 | 0.1 | 0.08 |
| 30 | m1 | 0.21 | 0.2 | 0.19 |
| | m2 | 0.16 | 0.15 | 0.16 |
| | m3 | 0.18 | 0.19 | 0.18 |
| | m4 | 0.17 | 0.16 | 0.17 |

Table 5.6 standard deviation of first object from P2

| force | movement | 1 | 2 | 3 |
|---|---|---|---|---|
| ww | m1 | 0.08 | 0.08 | 0.08 |
| | m2 | 0.07 | 0.07 | 0.07 |
| | m3 | 0.07 | 0.06 | 0.06 |
| | m4 | 0.05 | 0.05 | 0.047 |
| 10 | m1 | 0.1 | 0.1 | 0.1 |
| | m2 | 0.09 | 0.09 | 0.09 |
| | m3 | 0.09 | 0.09 | 0.09 |
| | m4 | 0.06 | 0.05 | 0.05 |
| 20 | m1 | 0.11 | 0.11 | 0.11 |
| | m2 | 0.11 | 0.11 | 0.1 |
| | m3 | 0.09 | 0.1 | 0.095 |
| | m4 | 0.08 | 0.08 | 0.07 |
| 30 | m1 | 0.16 | 0.15 | 0.15 |
| | m2 | 0.14 | 0.14 | 0.13 |
| | m3 | 0.1 | 0.11 | 0.1 |
| | m4 | 0.098 | 0.1 | 0.09 |

Table 5.7 standard deviation of second object from P1

| force | movement | 1 | 2 | 3 |
|---|---|---|---|---|
| ww | m1 | 0.09 | 0.1 | 0.09 |
| | m2 | 0.07 | 0.06 | 0.07 |
| | m3 | 0.09 | 0.08 | 0.08 |
| | m4 | 0.08 | 0.08 | 0.079 |
| 10 | m1 | 0.11 | 0.11 | 0.11 |
| | m2 | 0.08 | 0.08 | 0.07 |
| | m3 | 0.1 | 0.1 | 0.1 |
| | m4 | 0.1 | 0.1 | 0.1 |
| 20 | m1 | 0.13 | 0.12 | 0.12 |
| | m2 | 0.094 | 0.09 | 0.09 |
| | m3 | 0.12 | 0.12 | 0.11 |
| | m4 | 0.11 | 0.11 | 0.09 |
| 30 | m1 | 0.16 | 0.17 | 0.16 |
| | m2 | 0.11 | 0.1 | 0.1 |
| | m3 | 0.15 | 0.14 | 0.15 |
| | m4 | 0.13 | 0.13 | 0.12 |

Table 5.8 standard deviation of second object from P2

| force | movement | 1 | 2 | 3 |
|---|---|---|---|---|
| ww | m1 | 0.08 | 0.07 | 0.07 |
| | m2 | 0.05 | 0.05 | 0.06 |
| | m3 | 0.06 | 0.07 | 0.07 |
| | m4 | 0.05 | 0.04 | 0.05 |
| 10 | m1 | 0.09 | 0.08 | 0.08 |
| | m2 | 0.07 | 0.07 | 0.06 |
| | m3 | 0.07 | 0.06 | 0.07 |
| | m4 | 0.05 | 0.06 | 0.05 |
| 20 | m1 | 0.12 | 0.12 | 0.12 |
| | m2 | 0.11 | 0.11 | 0.11 |
| | m3 | 0.11 | 0.11 | 0.1 |
| | m4 | 0.09 | 0.08 | 0.08 |
| 30 | m1 | 0.15 | 0.14 | 0.14 |
| | m2 | 0.14 | 0.14 | 0.13 |
| | m3 | 0.12 | 0.13 | 0.12 |
| | m4 | 0.1 | 0.1 | 0.1 |

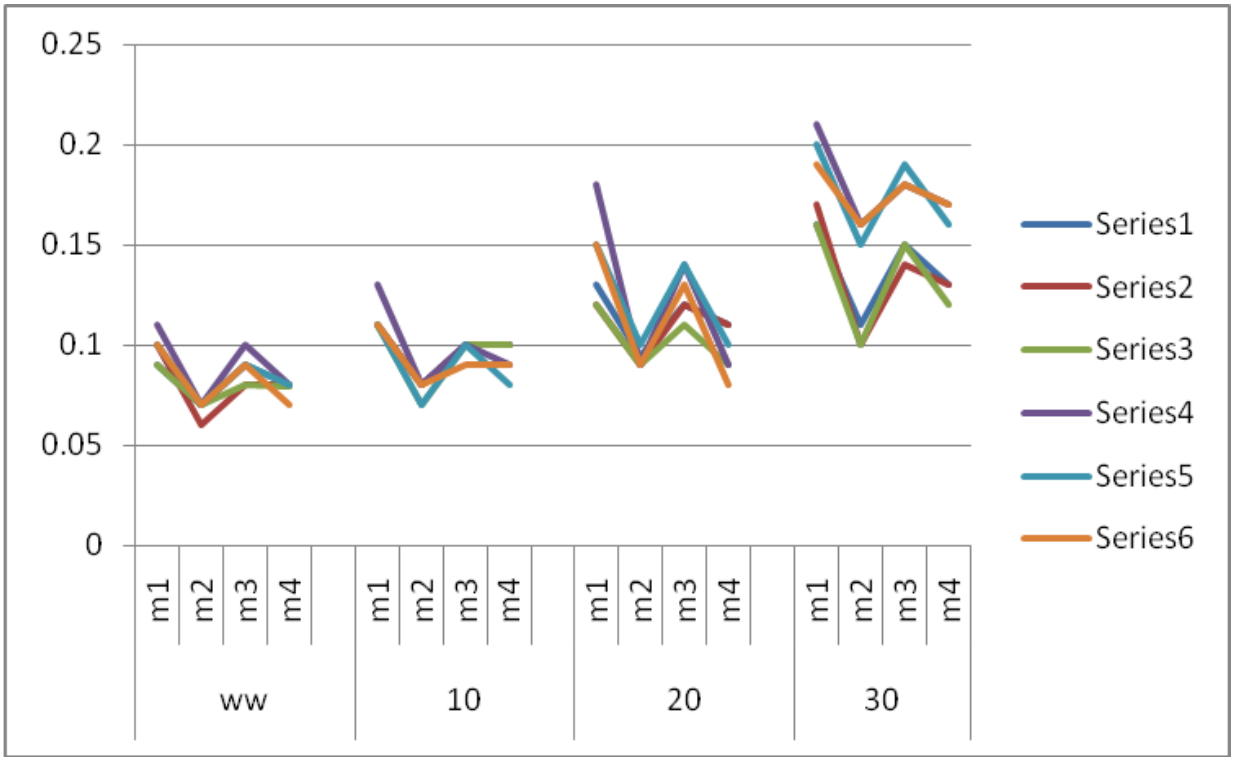


Fig. 5.5 Plot for P1 between standard deviation values vs different motions at different forces

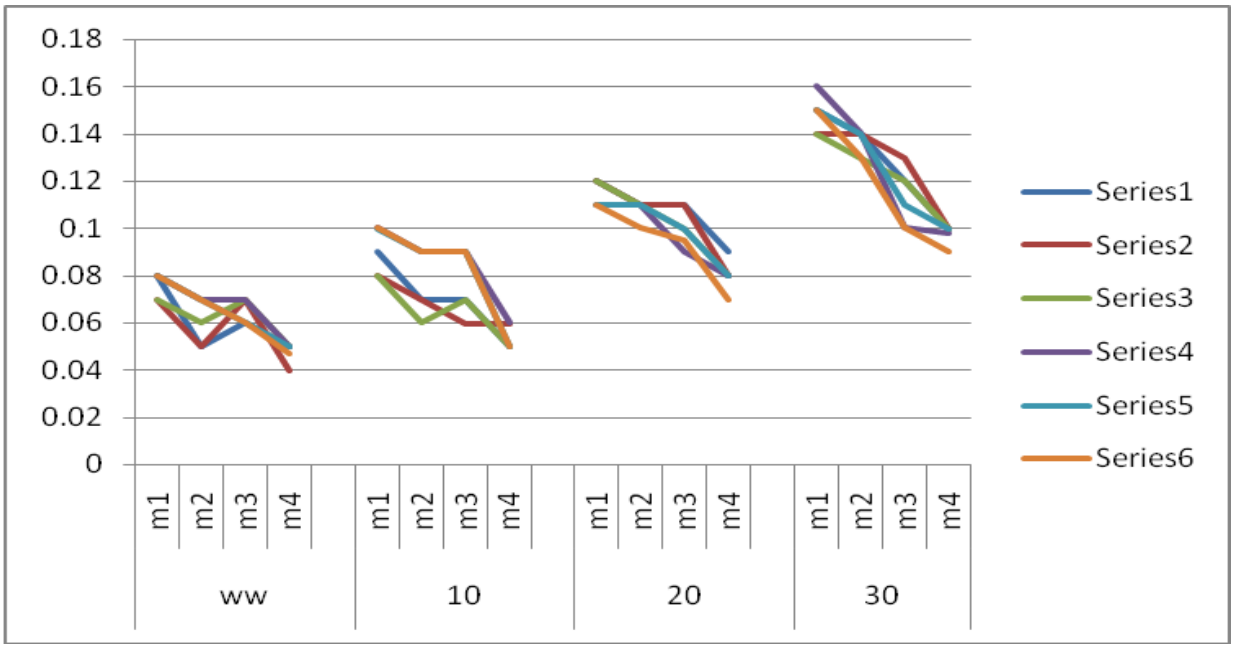


Fig. 5.6 Plot for P2 between standard values vs different motions at different forces

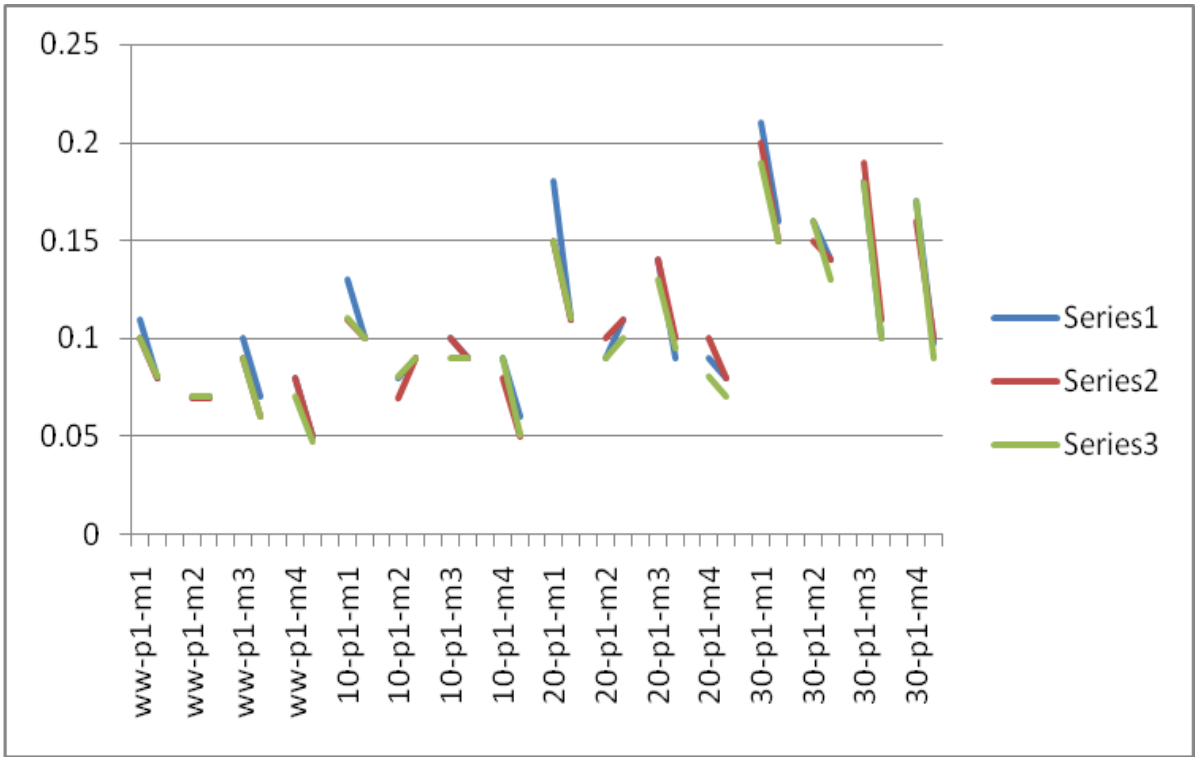


Fig. 5.7 Plot for standard deviation values for P1 and P2

## 5.2 For standard deviations

For the same observations, standard deviations (SD) of the SEMG signals were calculated. Fig. 5.5 shows the variation for 'P1' SD and different motions at different forces. It shows that the 'm1' has more SD than 'm2' and 'm3' has more SD than 'm4'. Fig. 5.6 shows the variation for 'P2' SD and different motions at different forces. Fig. 5.7 shows the variation for SD for P1 and P2. It shows that that P1 has more SD as compared to 'P2'. It means 'P1' is more dominating point.

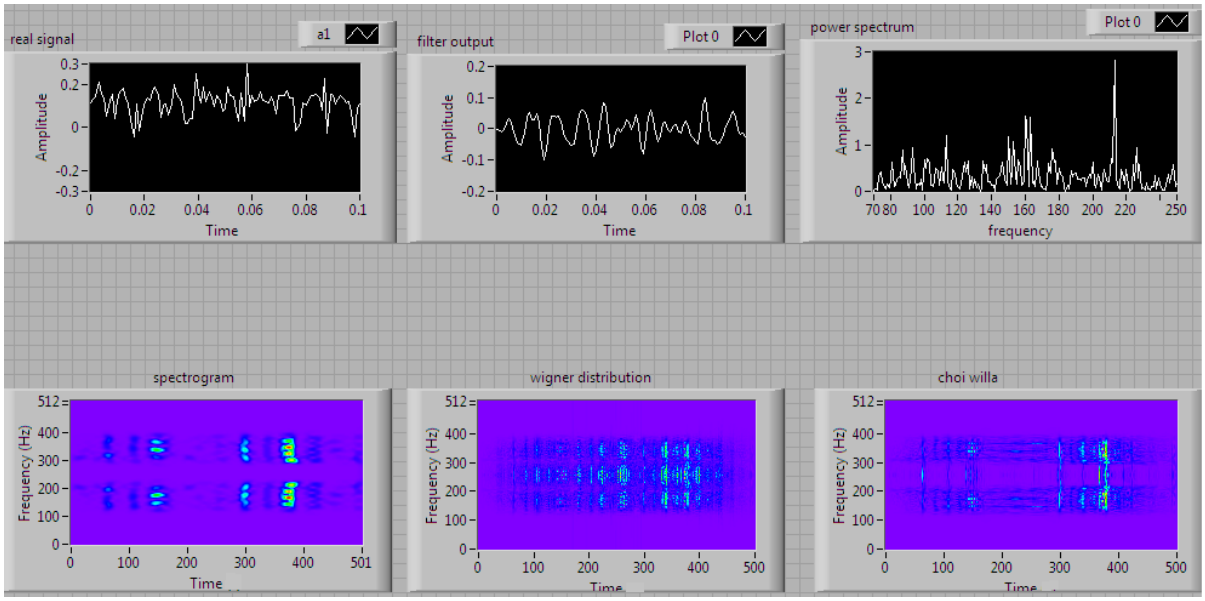


Fig. 5.8 Power spectrum, spectrogram, WVD and CWD for ‘m1’ without force

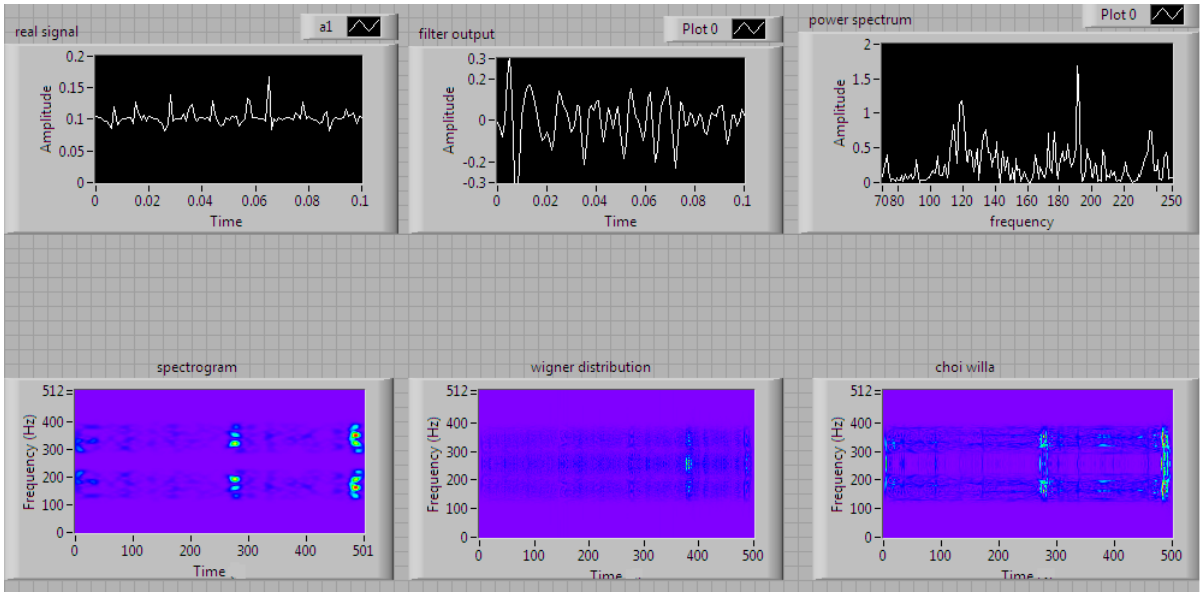


Fig. 5.9 Power spectrum, spectrogram, WVD and CWD for ‘m2’ without force

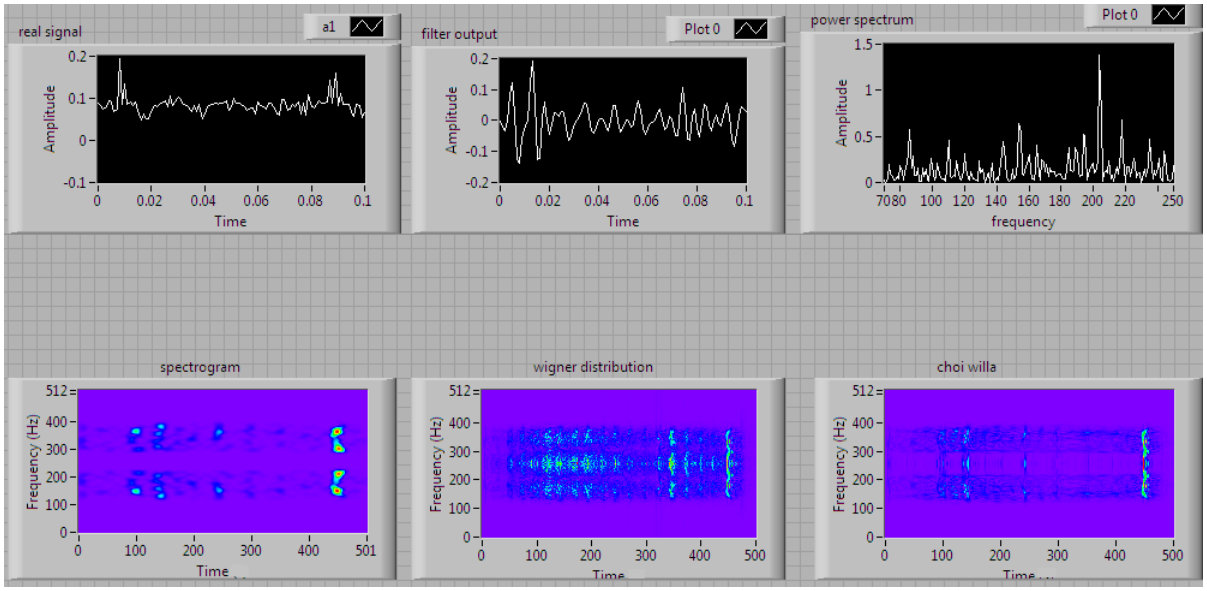


Fig. 5.10 Power spectrum, spectrogram, WVD and CWD for ‘m3’ without force

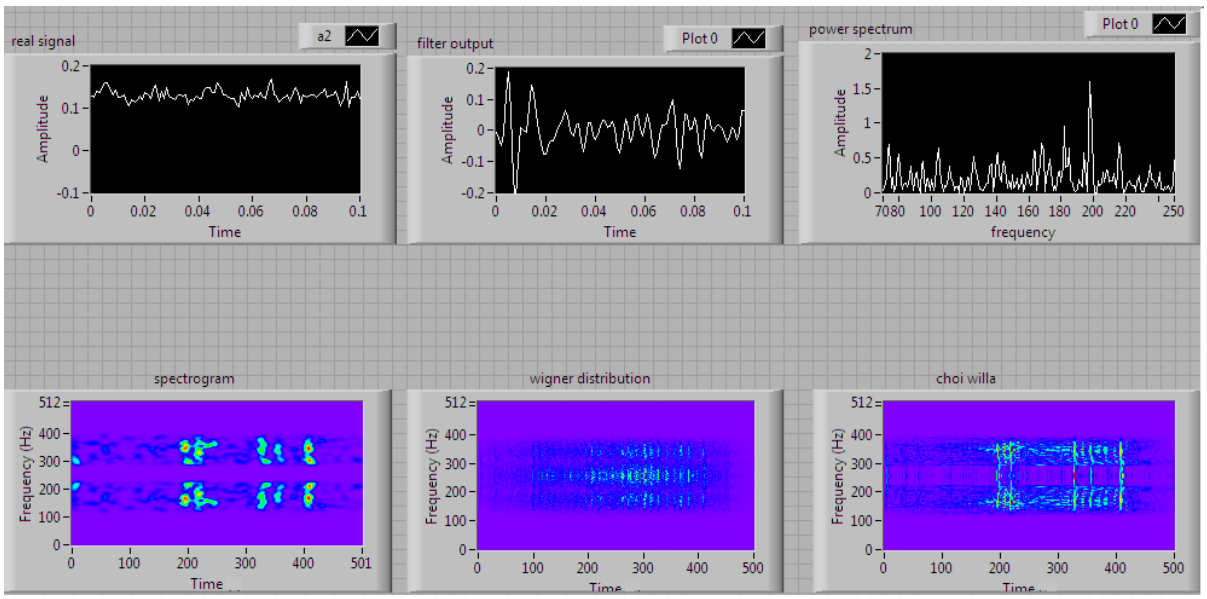


Fig. 5.11 Power spectrum, spectrogram, WVD and CWD for ‘m4’ without force

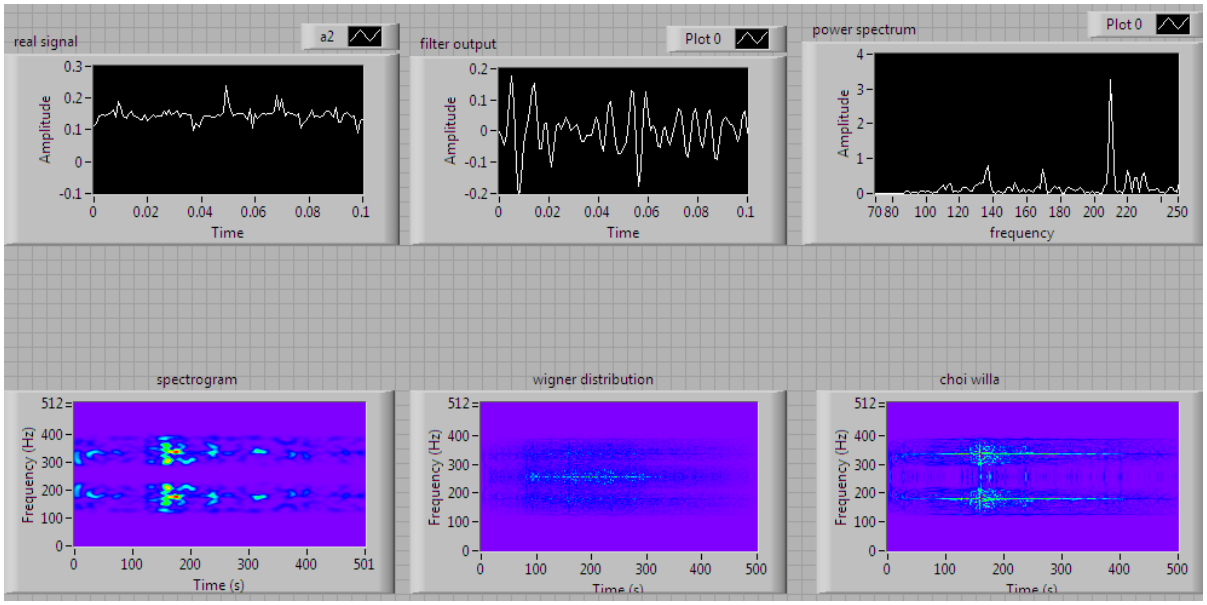


Fig. 5.12 Power spectrum, spectrogram, WVD and CWD for ‘m1’ at force ‘10’

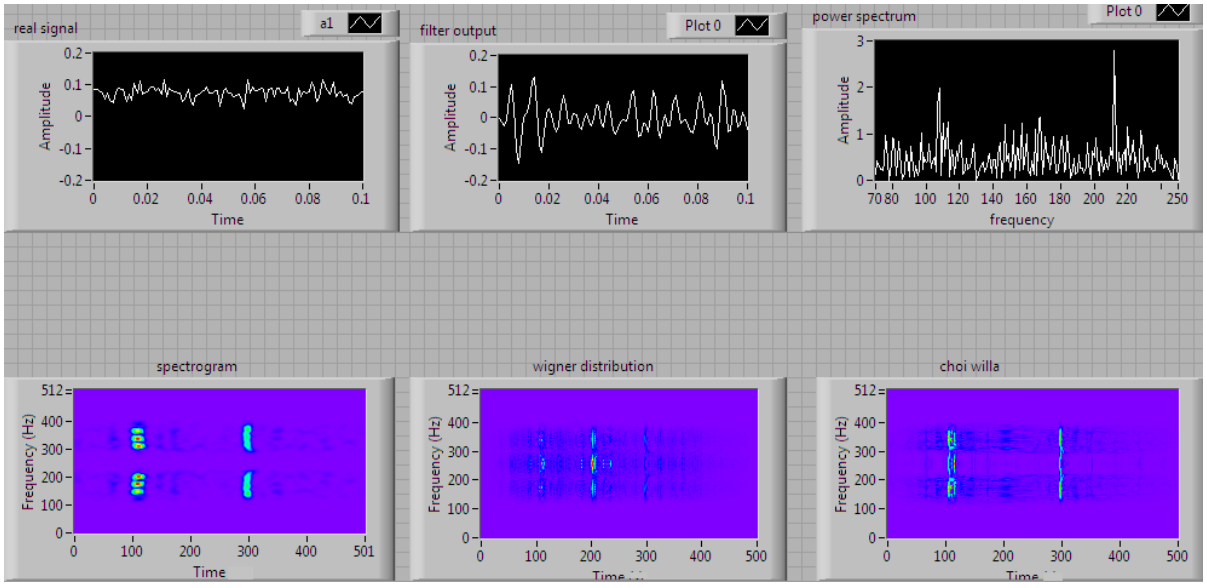


Fig. 5.13 Power spectrum, spectrogram, WVD and CWD for ‘m2’ at force ‘10’

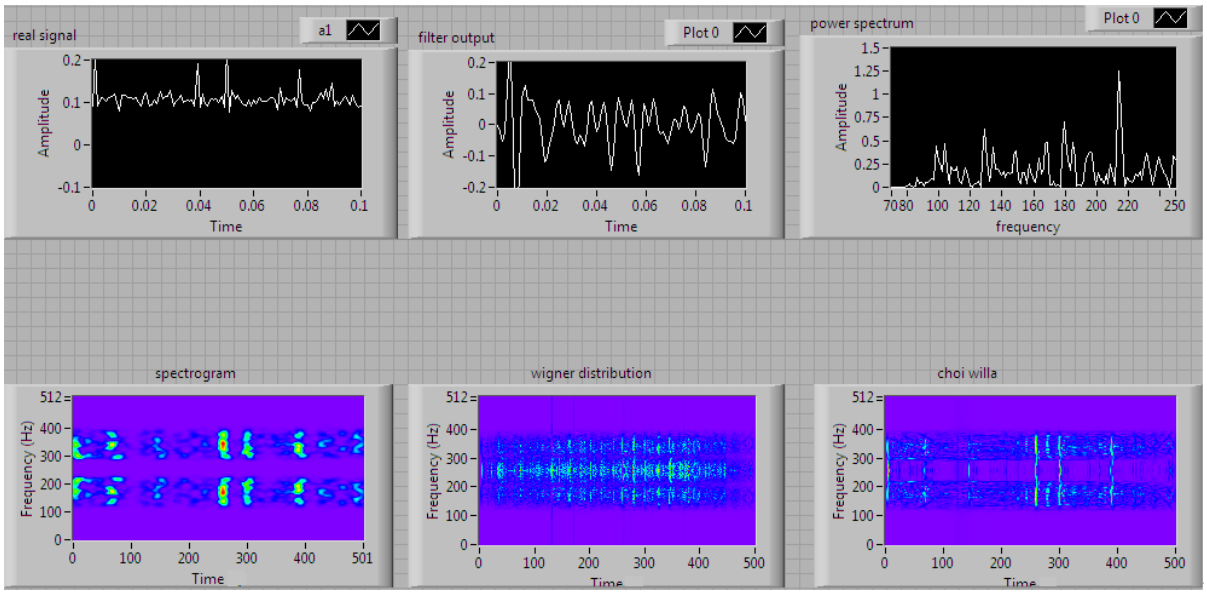


Fig. 5.14 Power spectrum, spectrogram, WVD and CWD for ‘m3’ at force ‘10’

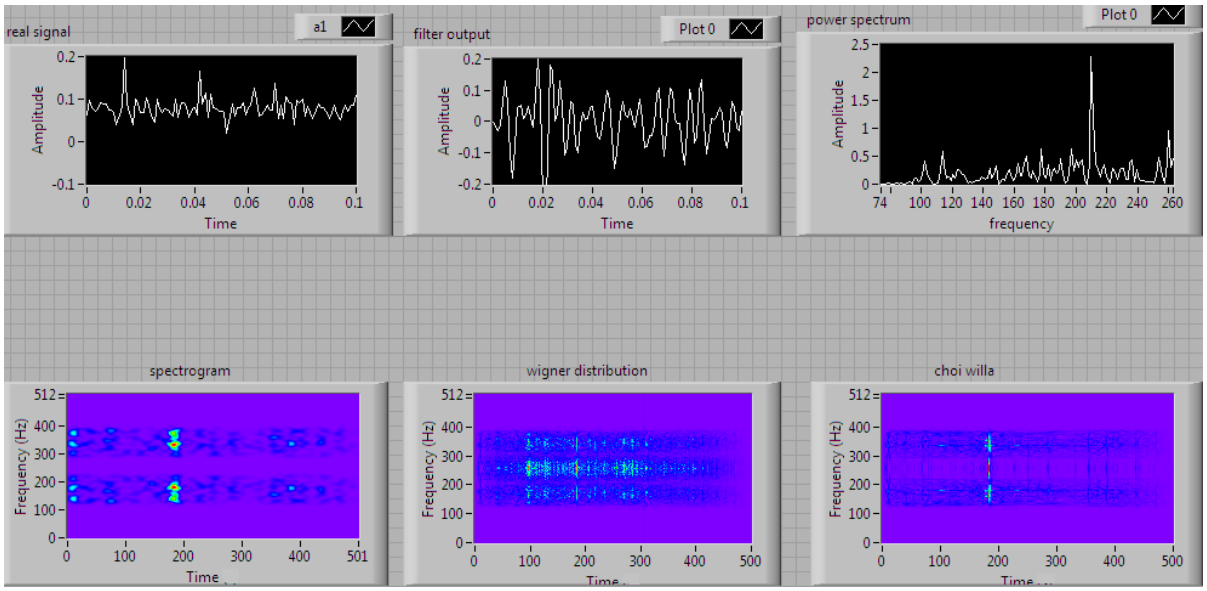


Fig. 5.15 Power spectrum, spectrogram, WVD and CWD for ‘m4’ at force ‘10’

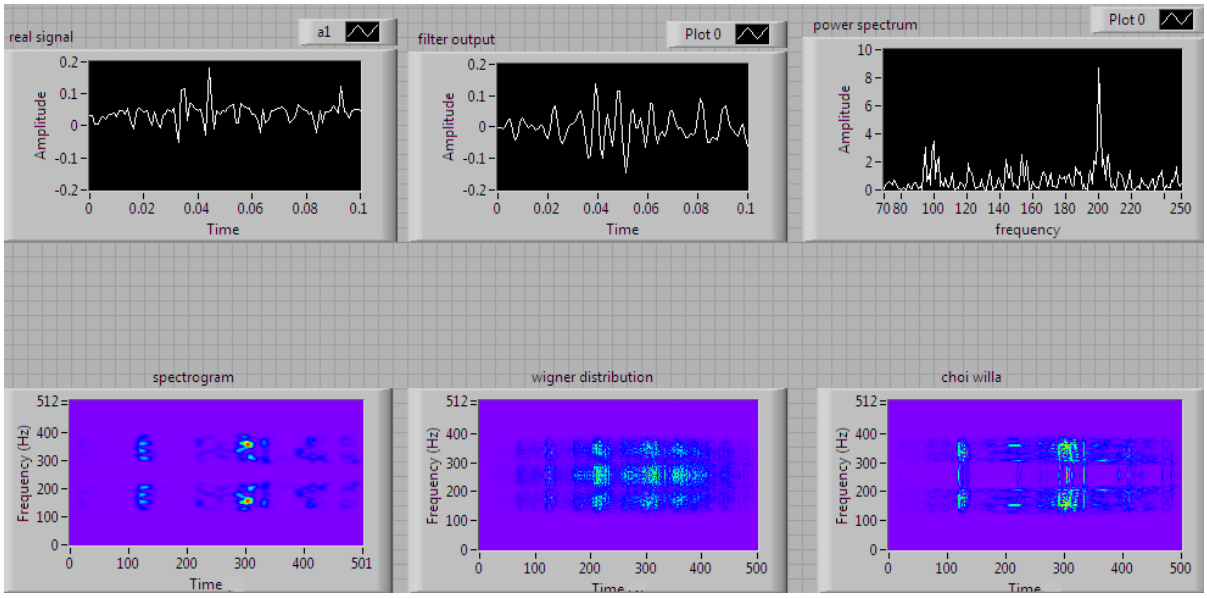


Fig. 5.16 Power spectrum, spectrogram, WVD and CWD for ‘m1’ at force ‘20’

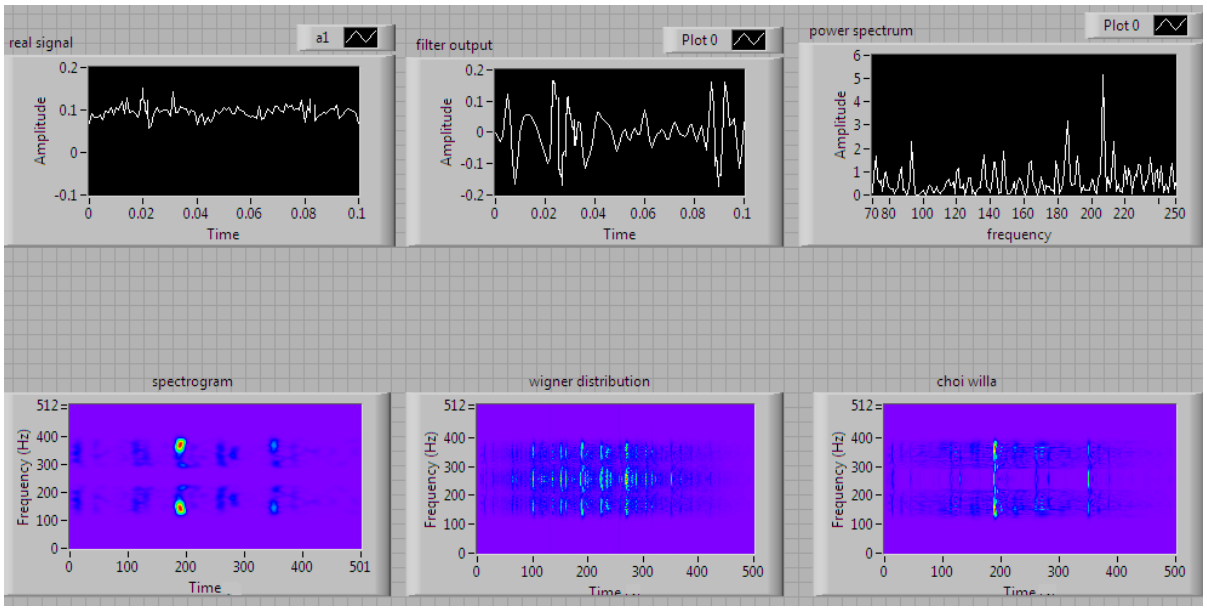


Fig. 5.17 Power spectrum, spectrogram, WVD and CWD for ‘m2’ at force ‘20’

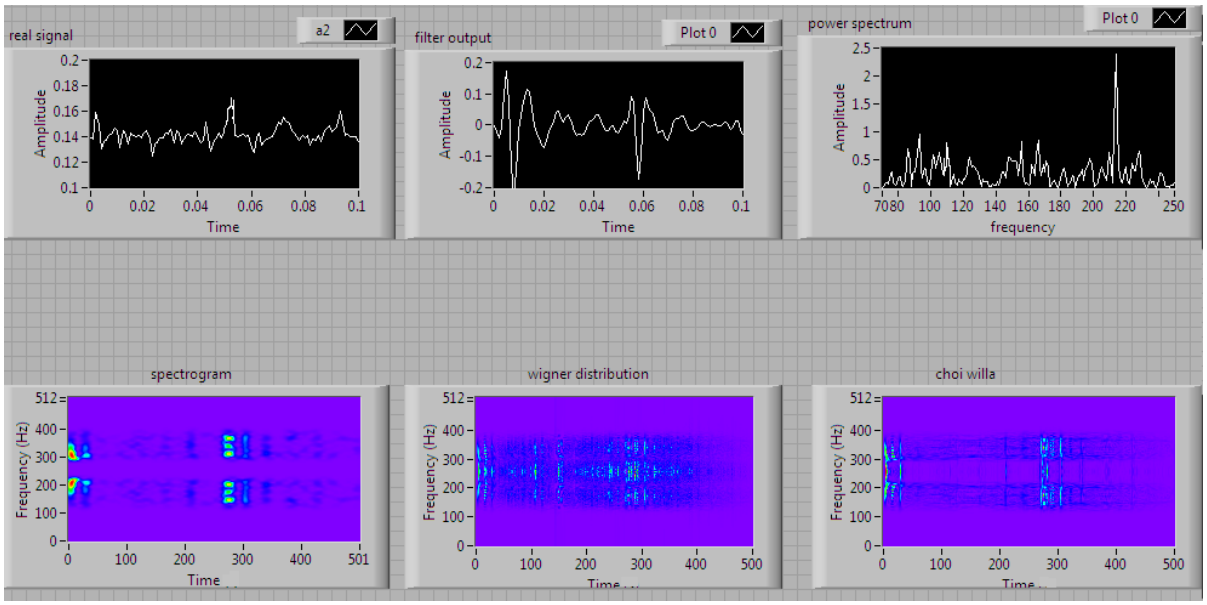


Fig. 5.18 Power spectrum, spectrogram, WVD and CWD for ‘m3’ at force ‘20’

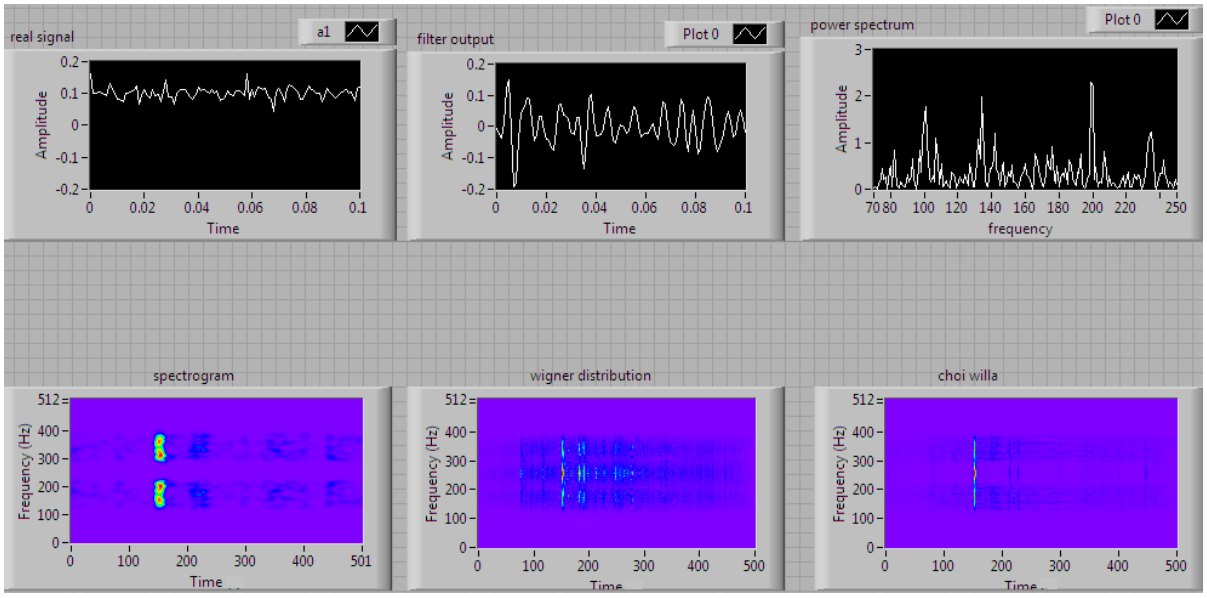


Fig. 5.19 Power spectrum, spectrogram, WVD and CWD for ‘m4’ at force ‘20’

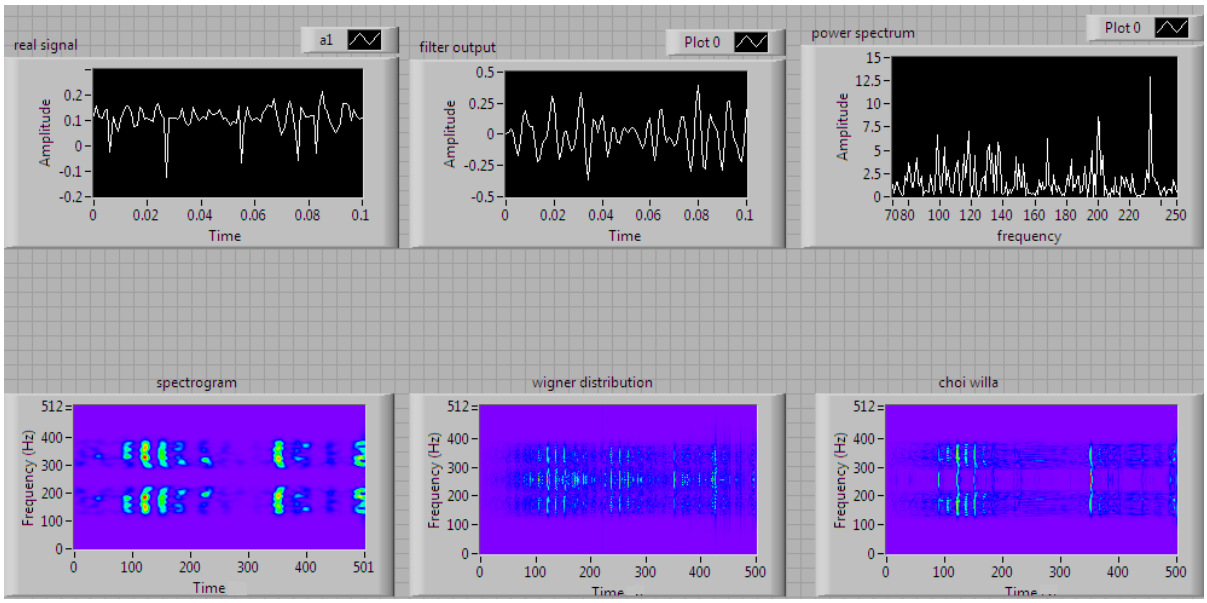


Fig. 5.20 Power spectrum, spectrogram, WVD and CWD for ‘m1’ at force ‘30’

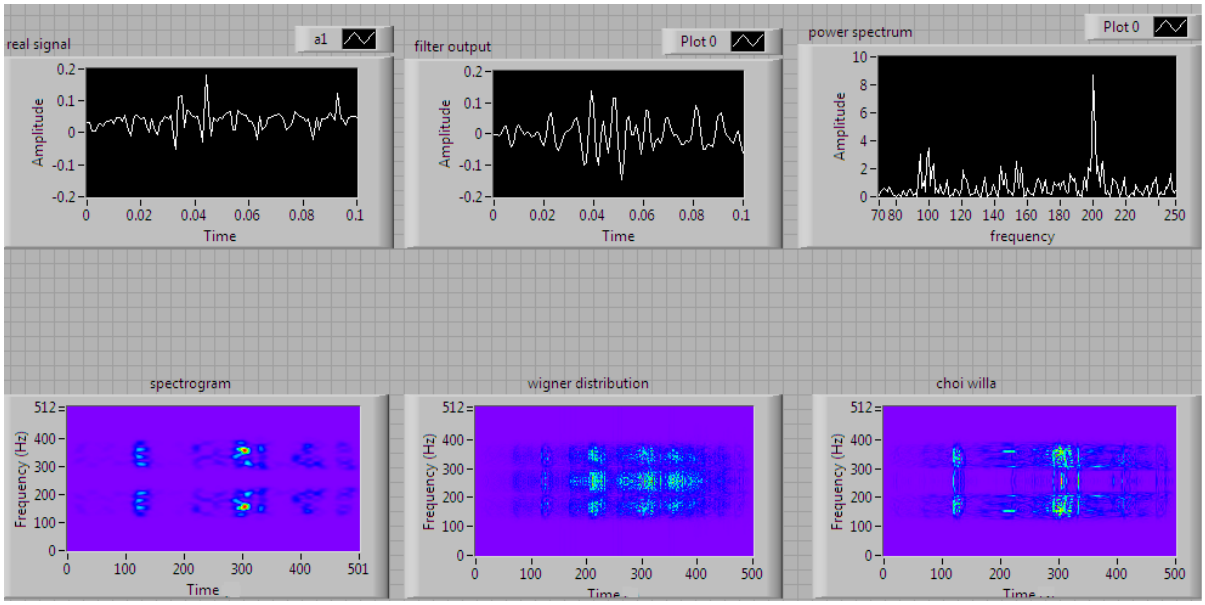


Fig. 5.21 Power spectrum, spectrogram, WVD and CWD for ‘m2’ at force ‘30’

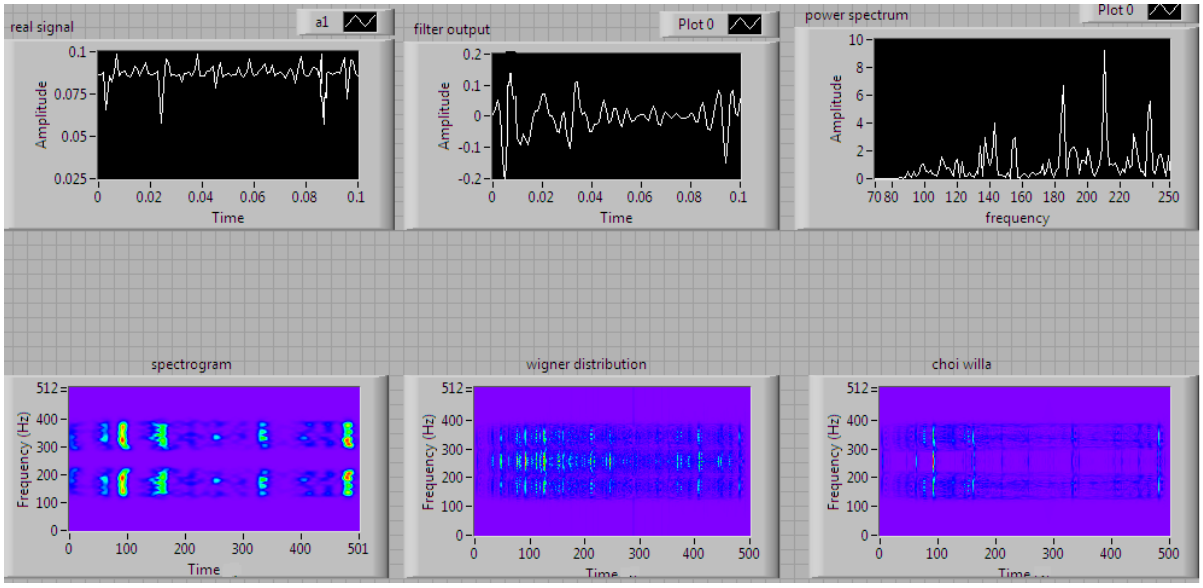


Fig. 5.22 Power spectrum, spectrogram, WVD and CWD for ‘m3’ at force ‘30’

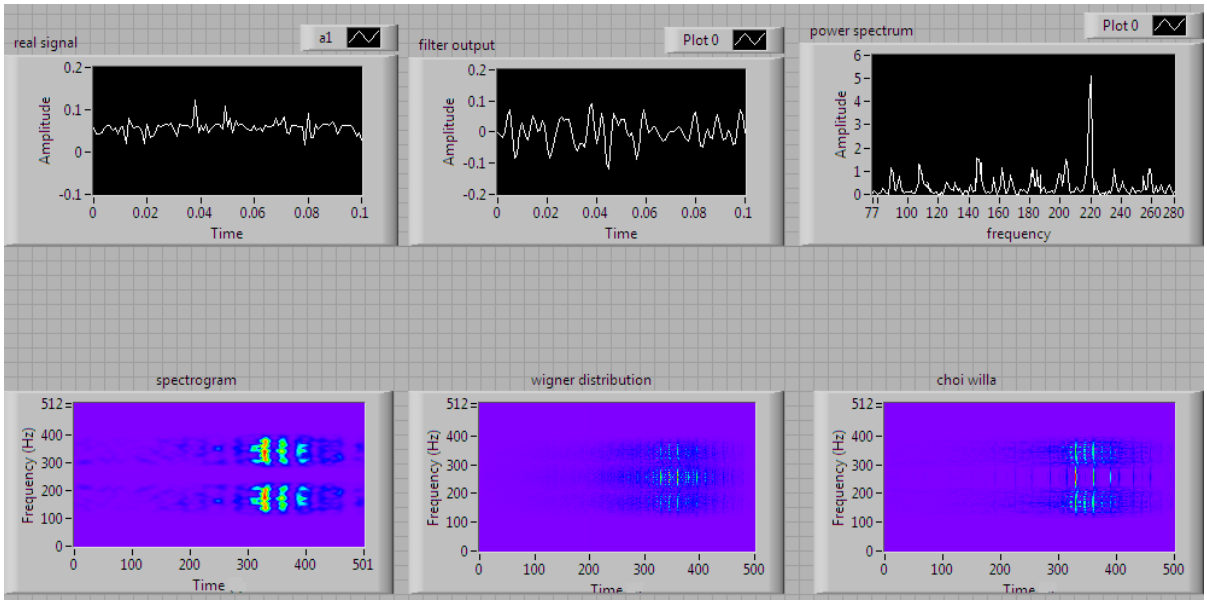


Fig. 5.23 Power spectrum, spectrogram, WVD and CWD for ‘m2’ at force ‘30’

Table 5.9 Force vs max freq. and magnitude

| | Max. frequency component | | | | magnitude | | | |
|---|---|---|---|---|---|---|---|---|
| f-0 | 214.1 | 191.5 | 204.2 | 198.3 | 2.82 | 2.19 | 1.5 | 1.77 |
| f-10 | 210.4 | 212.4 | 214.5 | 210.3 | 3.54 | 2.78 | 1.44 | 2.47 |
| f-20 | 199.6 | 206.7 | 214.2 | 198.8 | 9.37 | 5.49 | 2.58 | 2.23 |
| f-30 | 233.1 | 200.2 | 210.6 | 199.1 | 13.21 | 9.37 | 9.43 | 6.06 |

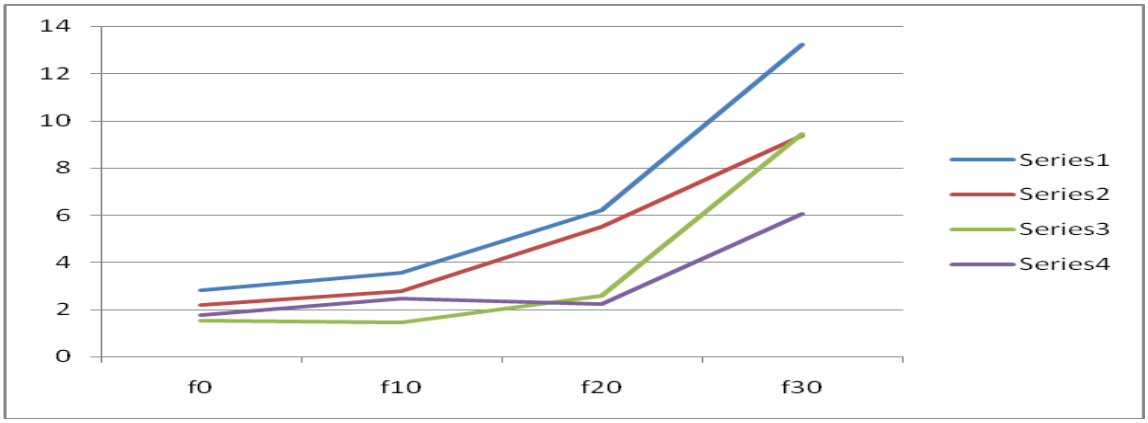


Fig. 5.24 Plot between force vs magnitude

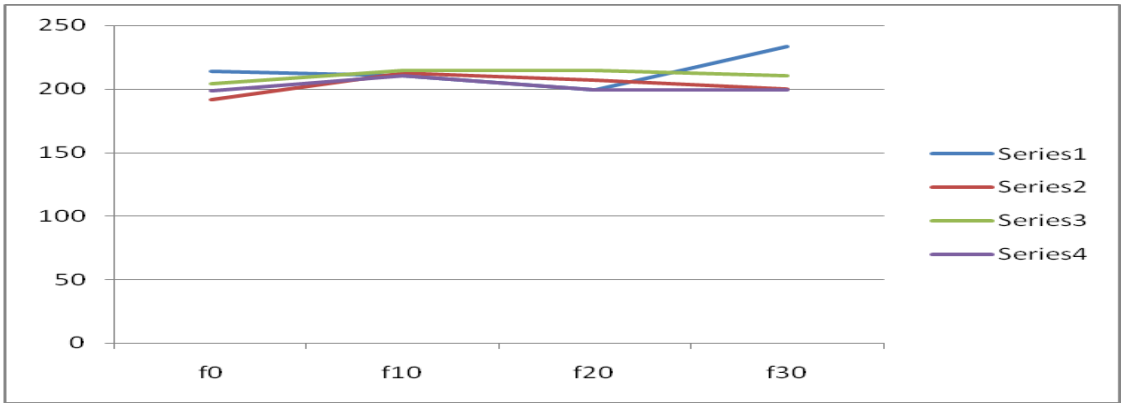


Fig. 5.25 Plot between force vs max. frequency

## 5.3 For power spectrum, spectrogram, WVD, CWD

Fig. 5.8-5.23 shows the power spectrum, spectrogram, WVD and CWD for different motions at different weight. Fig. 5.8 shows the power spectrum, spectrogram, WVD and CWD for 'm1' without force. Power spectrum shows that the maximum frequency of the signal is 214.1 Hz and its magnitude is 2.82. Spectrogram shows that the most dominant signal is

around frequency 200-220 Hz. WVD and CWD shows frequency variation with time and WVD is noisier. Fig. 5.9 shows the power spectrum, spectrogram, WVD and CWD for ‘m2’ without force. Power spectrum gives that the maximum frequency of the signal is 191.5 Hz and its magnitude is 2.19. Spectrogram shows that the most dominant signal is around frequency 180-210 Hz. WVD has more interference as compare to CWD. Fig. 5.10 shows the power spectrum, spectrogram, WVD and CWD for ‘m3’ without force. Power spectrum gives that the maximum frequency of the signal is 204.2 Hz and its magnitude is 1.50. Spectrogram shows that the most dominant signal is around frequency 200-220Hz. WVD is noisier as compare to CWD. Fig. 5.11 shows the power spectrum, spectrogram, WVD and CWD for ‘m4’ without force. Power spectrum gives that the maximum frequency of the signal is 198.3 Hz and its magnitude is 1.77. Spectrogram show that the most dominant signal is around frequency 190-220 Hz. CWD is has better frequency resolution.

Fig. 5.12 shows the power spectrum, spectrogram, WVD and CWD for ‘m1’ at force ‘10’. Power spectrum gives that the maximum frequency of the signal is 210.4 Hz and its magnitude is 3.54. Spectrogram shows that the most dominant signal is around frequency 200-220 Hz. WVD is noisier. Fig. 5.13 shows the power spectrum, spectrogram, WVD and CWD for ‘m2’ at force ‘10’. Power spectrum gives that the maximum frequency of the signal is 212.4 Hz and magnitude is 2.78. Spectrogram shows that the most dominant signal is around frequency 200-220 Hz. WVD has more interference as compare to CWD. Fig. 5.14 shows the power spectrum, spectrogram, WVD and CWD for ‘m3’ at force ‘10’. Power spectrum gives that the maximum frequency of the signal is 214.5 Hz and its magnitude is 1.44. Spectrogram shows that the most dominant signal is around frequency 200-220 Hz. CWD is has better frequency resolution. Fig. 5.15 shows the power spectrum, spectrogram, WVD and CWD for ‘m4’ at force ‘10’. Power spectrum gives that the maximum frequency of the signal is 210.3 Hz and its magnitude is 2.47. Spectrogram shows that the most dominant signal is around frequency 200-220Hz. WVD is noisier as compare to CWD.

Fig. 5.16 shows the power spectrum, spectrogram, WVD and CWD for ‘m1’ at force ‘20’. Power spectrum gives that the maximum frequency of the signal is 199.6 Hz and its magnitude is 6.22. Spectrogram shows that the most dominant signal is around frequency

190-220 Hz. WVD is noisier. Fig. 5.17 shows the power spectrum, spectrogram, WVD and CWD for ‘m2’ at force ‘20’. Power spectrum gives that the maximum frequency of the signal is 206.7 Hz and its magnitude is 5.49. Spectrogram shows that the most dominant signal is around frequency 200-220 Hz. WVD has more interference as compare to CWD. Fig. 5.18 shows the power spectrum, spectrogram, WVD and CWD for ‘m3’ at force ‘20’. Power spectrum gives that the maximum frequency of the signal is 214.2 Hz and magnitude is 2.58. Spectrogram shows that the most dominant signal is around frequency 200-220 Hz. CWD is has better frequency resolution. Fig. 5.19 shows the power spectrum, spectrogram, WVD and CWD for ‘m4’ at force ‘20’. Power spectrum gives that the maximum frequency of the signal is 198.8 Hz and magnitude 2.23. Spectrogram shows that the most dominant signal is around frequency 190-220Hz. WVD is noisier as compare to CWD.

Fig. 5.20 shows the power spectrum, spectrogram, WVD and CWD for ‘m1’ at force ‘30’. Power spectrum gives that the maximum frequency of the signal is 233.1 Hz and magnitude 13.21. Spectrogram shows that the most dominant signal is around frequency 200-240 Hz. WVD is noisier. Fig. 5.21 shows the power spectrum, spectrogram, WVD and CWD for ‘m2’ at force ‘30’. Power spectrum gives that the maximum frequency of the signal is 200.2 Hz and magnitude 9.37. Spectrogram shows that the most dominant signal is around frequency 190-220 Hz. WVD has more interference as compare to CWD. Fig. 5.22 shows the power spectrum, spectrogram, WVD and CWD for ‘m3’ at force ‘30’. Power spectrum gives that the maximum frequency of the signal is 210.6 Hz and magnitude is 9.43. Spectrogram shows that the most dominant signal is around frequency 200-220 Hz. CWD is has better frequency resolution. Fig. 5.23 shows the power spectrum, spectrogram, WVD and CWD for ‘m4’ at force ‘30’. Power spectrum gives that the maximum frequency of the signal is 199.1 Hz and magnitude 6.06. Spectrogram shows that the most dominant signal is around frequency 190-220 Hz. WVD is noisier as compare to CWD.

Fig. 5.24 shows the variation of force with magnitude which is almost linear. That is increasing with the increase of force. Fig. 5.25 refers that SEMG max. frequency remains between 195-235 Hz with the change of motion and force.

## 5.4 Conclusion

SEMG signals were taken by active electrodes between elbow and shoulder at acupressure points ‘P1’ and ‘P2’ at different forces (ww, 10 kg, 20 kg, and 30 kg). Signal was acquired in soft scope Labview by DAQ card (NI DAQ 6024E) and analyzed. Fig. 5.1 and Fig. 5.2 shows that up (m1) has high RMS value as compare to down (m2) and cw (m3) has high RMS value as compare to acw (m4). Fig. 5.3 shows that with the increase of force RMS values increase. Fig. 5.4 shows the difference between ‘P1’ and ‘P2’. It clearly indicates that ‘P1’ has high values as compare to ‘P2’ i.e., ‘P1’ is more dominating point.

Fig. 5.5 and Fig. 5.6, shows that up (m1) has high standard deviation as compare to down (m2) and cw (m3) has high standard deviation as compare to acw (m4) and with increase of force standard deviation increase. Fig. 5.7 shows the difference between ‘P1’ and ‘P2’. It clearly indicates that ‘P1’ has high standard deviation as compare to ‘P2’ i.e. ‘P1’ is more dominating point.

Power spectrum study shows that SEMG signals frequency remains between 190-235 Hz with the increase of force and with different movements while the magnitude of maximum frequency (2.82 to 13.21) increase with the increase of force. Fig. 5.8-5.23, WVD and CWD show the variation of frequency with time and show at which time signal is most dominant. Therefore, WVD has noisier, more interferences and less resolution as compare to CWD.

## 5.5 Future scope

- Signal can be observed from more locations.
- A model can be developed with extensive study.

# REFERENCES


[1] S. Schulz, C. Pylatiuk and G. Bretthauer. "A New Ultra light Anthropomorphic Hand" IEEE International Conference on Robotics and Automation Seoul, Korea. vol. 3, pp. 2437-2441, 2001

[2] http://www.ncbi.nlm.nih.gov/pmc/articles/PMC1455479

[3] http://www.scribd.com/doc/50625922/Techniques-of-EMG-signal-analysis

[4] Shahjahan Shahid, Jacqueline Walker, Gerard M. Lyons, Ciaran A. Byrne, and Anand Ishwanath Nene, "Application of Higher Order Statistics Techniques to EMG Signals to Characterize the Motor Unit Action Potential", IEEE Transactions on Biomedical Engineering, vol. 52, no. 7, pp. 1195-1209, 2005

[5] Federico Casolo, Simone Cinquemani, Matteo Cocetta, "Functional Design of A Transmission for A Myoelectric Elbow Prosthesis", World Congress on Engineering, London, U.K, vol. 3, 2008

[6] D. K. Kumar, A. Melaku, "Electrode Distance and Magnitude of SEMG", EMBSBMES Conference Houston, USA, 2002

[7] Lars H. Lindstrom, Robert I. Magnusson, "Interpretation of Myoelectric Power Spectra: A Model and Its Applications", IEEE Transactions on Biomedical Engineering, vol. 65, no. 5, pp. 653-662, 1977

[8] Foster B. Stulen, Carlo J. de luca, "Frequency Parameters of the Myoelectric Signal as a Measure of Muscle Conduction Velocity" IEEE transactions on Biomedical Engineering, vol. 28, no. 7, pp. 515-523, 1981

[9] David T. Gibbons, Micheal D. O'riain, Sebastien Philippe Auguste, "An Above-Elbow Prosthesis Employing Programmed Linkages" IEEE Transactions on Biomedical Engineering, vol. 34, no. 7, pp. 493-498, 1987

[10] Edward A. Clancy and Neville Hogan, "Multiple Site Electromyography Amplitude Estimation", IEEE Transactions on Biomedical Engineering, vol. 42, no. 2, pp.203-211, 1995

[11] R. Merletti, L. R. Lo Conte and D. Sathyan, "Repeatability of Electrically-Evoked Myoelectric Signals in the Human Anterior Muscle", Journal of Electromyography and Kinesiology, vol. 5, no. 2, pp. 67-80, 1995

[12] Paolo Bonato, Gianluca Gagliati, and Marco Knaflitz, "Analysis of Myoeletric Signal Recoded during Dynamic Contraction", IEEE Engineering in Medicine and Biology, vol. 39, no. 7, pp.102-111, 1996

[13] Bonato, P. D'Alessio, T. Knaflitz, M. Dipt. di Elettronica, Politecnico di Torino, "A Statistical Method for the Measurement of Muscle Activation Intervals from Surface Myoelectric Signal during Gait", IEEE Transactions on Biomedical Engineering, vol. 45, no. 3, pp. 287, 1998

[14] Z. Escudero, L. Leija, Ja. hvarez, R. Muiioz," Upper Limb Prosthesis Controlled by Myoelectric Signal", BMES/EMBS Conference Serving Humanity, Advancing Technology, Atlanta, GA, USA , pp. 636, 1999

[15] C. P. Fermo; C. V. De Vincenzo; T. F. Bastos-Filho; V. I. Dynnikov, "Development of an Adaptative Framework for the Control of Upper Limb Myoelectric Prosthesis", Annual EMBS International Conference, Chicago IL, pp.2402-2405, 23-28, 2000.

[16] Gerhard Staude, Claus Flachenecker, Martin Daumer, Werner Wolf, "Onset Detection in Surface Electromyographic Signals: A Systematic Comparison of Methods", EURASIP Journal on Applied Signal Processing, vol. 2, pp. 67– 81, 2001

[17] S. Venkataramanan, N.V. Kalpakam, A. Samant. "Optimization Analysis of Intelligent Myoelectric Control", second IEEE International Conference on Intelligent Systems, pp. 474-479, 2004

[18] Wendy Franks, Iwan Schenker, Patrik Schmutz, Andreas Hierlemann, "Impedance Characterization and Modeling of Electrodes for Biomedical Applications", IEEE Transactions on Biomedical Engineering, vol. 52, no. 7, 2005

[19] Yuet-Ming Lam, Philip Heng-Wai Leong, Man-Wai Mak, "Frame-Based SEMG-to-Speech Conversion", IEEE Transactions on Biomedical Engineering, vol. 1, pp. 173-17, 2006.

[20] Mahdi Khezri, Mehran Jahed, "A Novel Approach to Recognize Hand Movements via SEMG Patterns", IEEE International Conference EMBS Cité Internationale, Lyon, France 2007.

[21] M. B. I. Reaz, M. S. Hussain and F. Mohd-Yasin," Techniques of EMG Signal Analysis: Detection, Processing, Classification and Applications", IEEE Transactions on Biomedical Engineering, vol. 10, pp. 11-35, 2006

[22] Dapeng Yang, Jingdong Zhao, Yikun Gu, Li Jiang, Hong Liu," Estimation ofHand Grasp Force based on Forearm Surface EMG", IEEE International Conference on Mechatronics and Automation, Changchun, China, pp. 1795-1799, 2009

[23] Dr. Scott Day, "Important Factors in Surface EMG Measurement", Bortec Biomedical Ltd., pp. 7-10, 2009

[24] Yutaro Kobayashi, Osamu Fukayama, Takafumi Suzuki, Kunihiko Mabuchi, "Estimation of Finger Postures to Control a Maniform Device for Playing a Trumpet using Electromyographic Signals with External Triggers", IEEE International Conference EMBS Buenos Aires, Argentina, 2010

[25] Ryait H. S., Arora A. S. and Agarwal Ravinder, "Interpretations of Wrist Operations from Surface-EMG Signals at Different Locations on Arm along with Acupressure Points", IEEE Transactions on Biomedical Circuits and Systems, vol. 4, no. 2, pp. 101-111, 2010

[26] Irena Orovi´c, Milica Orlandi´c, Srdjan Stankovi´c, Zdravko Uskokovi´c, "A Virtual Instrument for Time-Frequency Analysis of Signals With Highly Non stationary Instantaneous Frequency", IEEE Transactions on Instrumentation and Measurement, vol. 60, no. 3, pp. 791-803, 2011

[27] http://www.ehow.com/how_4809043_pressure-points-arm-body.html